Designing self-amplifying replicons for transient gene expression of interleukin-18

Designing self-amplifying replicons for transient gene expression of interleukin-18

Simon Liang

A Thesis in the Field of Bioengineering and Nanotechnology

for the Degree of Master of Liberal Arts in Extension Studies

Harvard University

May 2021

Abstract

RNA-based therapeutics are on the rise as a re-emerging technology bolstered by the SARS-CoV-2 pandemic. However, issues such as storage, protein expression, and delivery are major challenges for the broad applicability. To address this issue, non-viral RNA replicon delivery systems can induce transient gene expression of immunomodulators and open the door to numerous potential targets that were once not viable due to dose-limiting toxicities affecting safety and efficacy. To that end, this work targets IL-18, a pleiotropic proinflammatory cytokine, which has been primarily viewed as a prognostic marker of various diseases like atherosclerosis, arthritis, diabetes, and cancer. In combination with another cytokine (IL-12), IL-18 is capable of enhancing the production of IFN-γ critical for anti-tumor immune responses. First, the synthesis of RNA replicons through *in vitro* transcription, characterization, and validation of IL-18 RNA replicons is described. Next, IL-18 RNA replicons are encapsulated in lipid nanoparticles and their function is analyzed using a melanoma cell line. Lastly, evidence of synergy between RNA replicons encoding for both IL-18 and IL-12 is shown through the production of robust IFN-γ responses in B16F10 co-cultures with naïve splenocytes. These studies provide a fundamental understanding to observe transient gene expression and synergy of dual expressing cytokines. Lastly, this system has the potential to be a promising tool for cancer immunotherapy.

Frontispiece

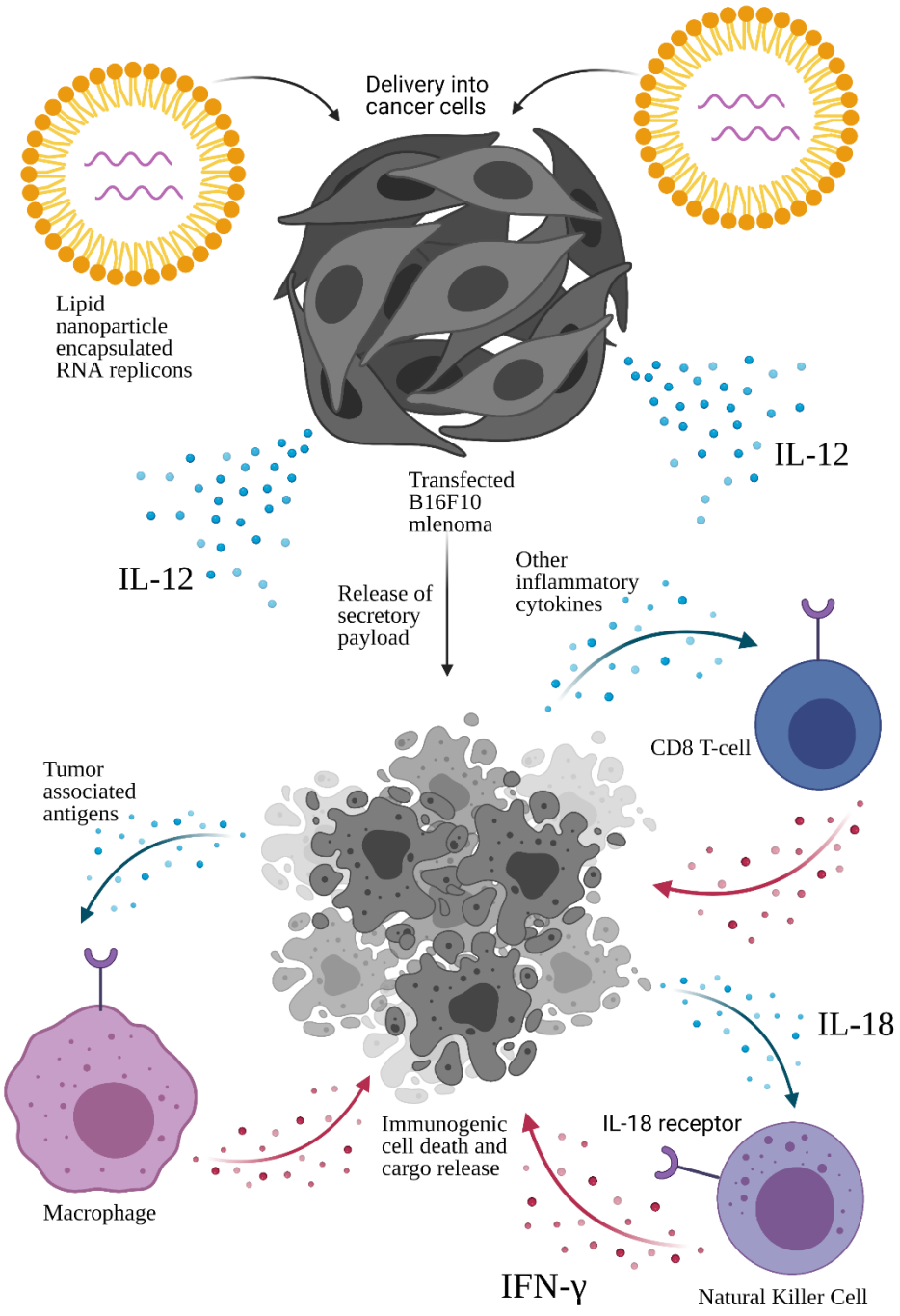

Made in Biorender.com

Dedication

To my beloved grandmother who passed away on April 14th, 2020 in Chicago due to complications with Type I diabetes during the COVID-19 pandemic. I will never forget your love, strength, and resilience. May you rest in peace.

To my supportive partner, Nathan Donahue, who has given me much joy on this journey in the pursuit of scientific inquiry and life of the mind. I love you.

Acknowledgments

First and foremost, I would like to thank, Professor Darrell Irvine, an Investigator of the Howard Hughes Medical Center, for his guidance, expertise, and for giving me the opportunity to conduct research in his laboratory. Many thanks for the constructive comments, patience, flexibility, and encouraging conversations that will continue to push me forward as I advance my career in the sciences. I am also extremely thankful to Mariane Melo for her never-ending guidance and support as a supervisor, mentor, and friend. I would also like to thank my research advisor Steven Denkin at the Harvard Extension School who has guided my writing and academic pursuits.

My heartfelt thanks go to the postdoctoral researchers, technical staff, and graduate students of the Irvine laboratory who I have gotten to know better and consider not only as colleagues but friends. I would like to give special thanks without whom this thesis would not have been possible, especially Yingzhong Li, Leyuan Ma, Parisa Yosefpour, Byungji Kim, Laura Maiorino, Murillo Silva, Sasan Jalili Firoozinezhad, Chensu Wang, Brittany Hartwell, Aereas Aung, Coralie Backlund, Lauren Milling, Sachin Bhagchandani, Heikyung Suh, Wuhbet Abraham, Na Li, Ina Sulkaj, and Dan Garafola. In particular, Tanaka Remba for help with the synthesis of the replicons for my experiments.

Also, thank you to the Koch Institute Flow Core facilities and Massachusetts Institute of Technology administrative staff who have made it possible for me to progress my research. Specifically, I would like to thank Mark Miller, Mariann Murray, Valerie Corapi, Idulia Lovato, and the staff at the MIT International Student's Office.

Moreover, I would like to thank my mentors for fruitful and inspiring conversations both scientifically and beyond. In particular, Bret Ulery, Renée F. de Pooter, and Kelly Moynihan for giving me sound advice and always lending an ear.

Table of Contents

List of Tables

List of Figures

Chapter I.

Introduction

RNA: A re-emerging technology in oncology

The age of RNA in cancer immunotherapy

In recent years, synthetic ribonucleic acids (RNAs) have reached technological milestones which have benefited our understanding of human disease, especially within the field of cancer immunotherapy or what is also known as immuno-oncology. A historic RNA milestone occurred during the COVID-19 pandemic caused by the spread of the severe acute respiratory syndrome coronavirus 2 (SARS-CoV-2) originating from Wuhan, China that led to the deaths of at least 2.54 million people globally (*WHO Coronavirus (COVID-19) Dashboard*, n.d.). In the United States, the Food & Drug Administration (FDA) granted an Emergency Use Authorization on December 11th, 2020 to Pfizer-BioNTech for a messenger RNA (mRNA) vaccine encoding for the coronavirus spike protein that mediates binding of the virus to host cells (Belouzard et al., 2012). The goal of this vaccine was to educate immune cells, the body's natural defense mechanism, to prevent severe disease onset. Pfizer-BioNTech demonstrated that their mRNA vaccine was able to elicit protective antibodies with approximately 95% efficacy in reducing SARS-CoV-2 infections (Polack et al., 2020). Concurrently, Moderna, in collaboration with the National Institutes of Health, demonstrated similar efficacy with their mRNA vaccine that encodes for a different part of the spike protein and received an Emergency Use Authorization from the FDA on December 19th, 2020 (Baden et al., 2021). These two

exciting authorizations paved the path forward to the resurgence and public interest in RNA research and therapies. Outside of preventative vaccine development, numerous companies are working on delivering RNA to combat debilitating chronic diseases like HIV and cancer (Blakney et al., 2021; Genentech, Inc., 2021a, 2021b).

Investigators have utilized different forms of nucleic acid vaccines so the technology is far from novel on its own. Earlier studies of gene therapy have been conducted using DNA due to its storage stability and feasibility to mass produce as opposed to RNA (C. Zhang et al., 2019). Unfortunately, DNA vaccines performed poorly in clinical trials due to the difficult requirement of DNA needing to enter the nucleus and concerns of genome integration causing permanent unwanted side effects (Kutzler & Weiner, 2008). On the other hand, a major advantage of RNA is that it does not require nuclear entry and allows for transient expression of antigenic peptides or proteins within the cytosol (Geall et al., 2012; Pascolo, 2008). RNA comes in many different shapes and flavors. The most extensively studied RNAs are heavily involved in protein synthesis which include mRNA, transfer RNA, and ribosomal RNA (Lodish et al., 2000). Also, some RNAs affect gene regulation by post-transcriptional modifications known as regulatory RNAs like small interfering RNA, short hairpin RNA, antisense RNA, and many more (Erdmann et al., 2001). These different flavors of RNA provide investigators a vast tool kit to test monotherapies and combination therapies, albeit not without challenges.

A major challenge that many RNA therapeutics face is the delivery vehicle used to get RNA into the target cell and cytosolic access (Donahue et al., 2019). This is due to enzymes that catalyze the degradation of RNA called RNases present in the surrounding environment that are responsible for the fast clearance of these modalities (Wadhwa et al.,

2020). To circumvent the degradation of RNA, various encapsulation methods have been pursued to improve the biodistribution of RNA therapies through the use of synthetic materials like lipid-based nanoparticles (Pardi et al., 2015). Another limitation is that RNA—particularly mRNA— may not generate potent responses on its own as strong and durable responses depend on the number of mRNA transcripts delivered to cells (Fuller & Berglund, 2020; Vogel et al., 2018). To that end, self-amplifying non-viral RNA replicon vaccines have been developed. These next-generation RNA platforms utilize self-replicating single-strand RNA virus machinery to produce multiple copies of the gene/protein of interest without generating infectious progeny unlike traditional viral particles (Geall et al., 2012; Lundstrom, 2018). A more detailed analysis of self-amplifying RNA replicons will be discussed later in this introductory chapter.

How has RNA revolutionized oncology and cancer immunotherapy? Traditionally, standard of care in the clinic relies on chemotherapy and surgical removal of the bulk malignancy, if possible. An emerging approach to cancer treatment—immunotherapy—does not treat cancer, but primarily targets the immune system to elicit an anti-tumor response against cancer cells (Moynihan, 2017). Utilizing self-amplifying RNA replicons that encode for a gene of interest is an advantageous strategy over traditional transient expression systems. This strategy will allow for the gene of interest to be translated into protein continuously *in situ* rather than administrating recombinant proteins directly which may have dose-limiting toxicities compared to endogenous production controlled by pre-existing thresholds and biological limits. Moreover, self-amplifying RNA replicons can prolong protein production without the adverse side effect of permanent expression which

is a major concern for long-term safety. Overall, RNA replicons have the potential to revolutionize immunotherapy.

A brief overview of design strategies of replicons

What is a "replicon"?

Replicons—specifically RNA replicons—are RNA molecules that form at a single origin of replication site (Kittell & Helinski, 1993). The origin of replication is the site of initiation, the first step in DNA and RNA replication. Viruses are notorious for their ability to replicate after infecting a host cell's machinery. A particularly interesting class of RNAs are derived from alphaviruses, which encode on their RNA genome a set of proteins that comprise an RNA-dependent RNA polymerase, which copies the RNA genome of the virus within the host cell (Lundstrom, 2014).

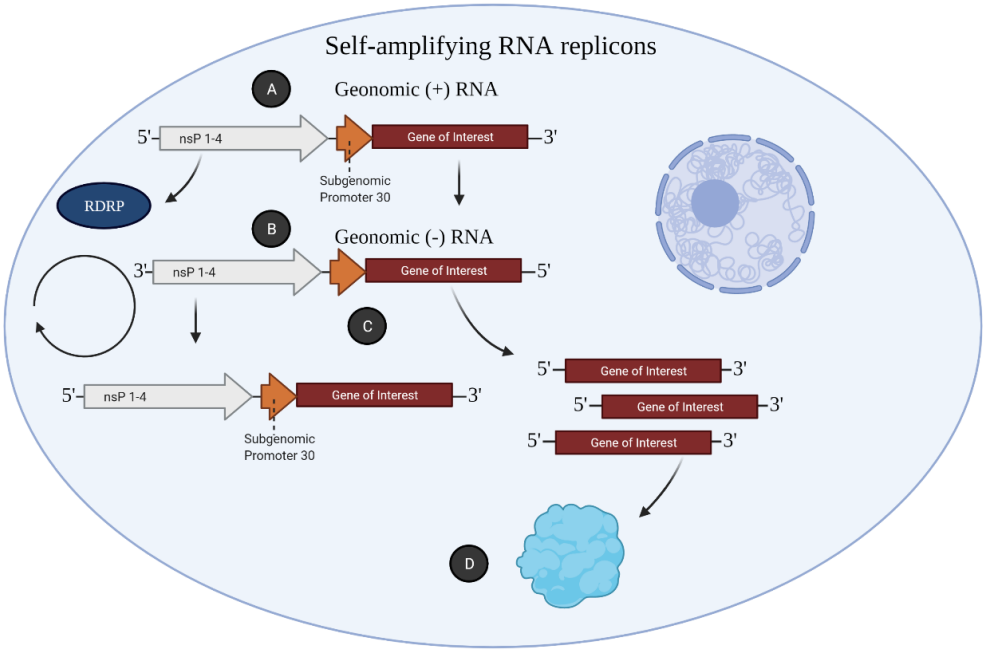

Figure 1. Overview of self-amplifying RNA replicon mechanism

A. *After cytosolic entry into the cell, RDRP replicase complex forms from the non-structural proteins 1-4.* ***B.*** *Replication of copies of self-amplifying RNA replicons from the positive sense genomic RNA to a negative sense RNA template.* ***C.*** *More copies of genomic positive sense RNA are made and subgenomic RNA.* ***D.*** *Translation of subgenomic RNA into multiple copies of the protein. Made with Biorender.com*

Compared to DNA in the nucleus responsible for storing genetic information, RNA is typically a single-stranded molecule that consists of adenine, uracil, cytosine, and guanine nucleic acids responsible for the translation of genetic information (i.e. genes of interest) into proteins (Figure 1). RNA replicons are capable of inducing high levels of transient gene expression which allows for specific genes of interest to be turned on for a short duration of time upon delivery into the cell cytosol (Geall et al., 2012).

The use of RNA replicons for drug delivery and vaccinations is an ongoing and growing field (Lundstrom, 2014). RNA replicons are made from disabled alpha- or flaviviruses unable to produce infectious progeny (McCullough et al., 2014). All alphaviruses and flaviviruses that cause disease are classified as arthropod-borne viruses (arboviruses) varying in structure and function (Hernandez et al., 2014). Alphaviruses are single-stranded RNA viruses with an envelope structure belonging to the *Togaviridae* family of viruses like the Semliki Forest virus or the Venezuelan equine encephalitis virus which are associated with epidemics in Central Africa and South America respectively (Lundstrom, 2014). *Flaviviridae* is a family of positive, single-stranded, enveloped RNA viruses heavily responsible for mosquito-transmitted diseases such as yellow fever, dengue fever, hemorrhagic fever, Zika virus, and West Nile virus (Gould & Solomon, 2008).

Each virus is differently configured where alphaviruses have non-structural genes under the genomic promoter (i.e. SP6 or T7 bacteriophage promoter) at the 5’ end followed

by structural genes under a subgenomic promoter at the 3' end. Flaviviruses, however, are expressed as a single polypeptide with the non-structural genes downstream of the gene of interest, opposite of alphaviruses, with a capped 5' terminus that is not polyadenylated whereas the 3' terminus is not polyadenylated forming a loop structure (Lundstrom, 2018). This body of work will primarily be exploring RNA replicons using the alphavirus structural format and its potential uses.

Structure and function of replicons: mechanism of action

There are three possible expression systems denoted as DNA layered systems, replication-proficient systems, and replication-deficient systems that exist (Lundstrom, 2014). DNA layered systems are plasmid vectors carrying either the full-length viral genome or nonstructural genes and the gene of interest all downstream of a cytomegalovirus promoter to synthesize DNA replicons. Replication-proficient systems contain both the structural genes and nonstructural genes and the gene of interest whereas replication-deficient only contain one or the other (Lundstrom, 2014). This section will be focusing on primarily replication-deficient replicon systems because they allow for the ability to transiently express genes of interest without danger of host integration (unlike DNA layered systems) and do not generate viral infectious particles like replication-proficient systems.

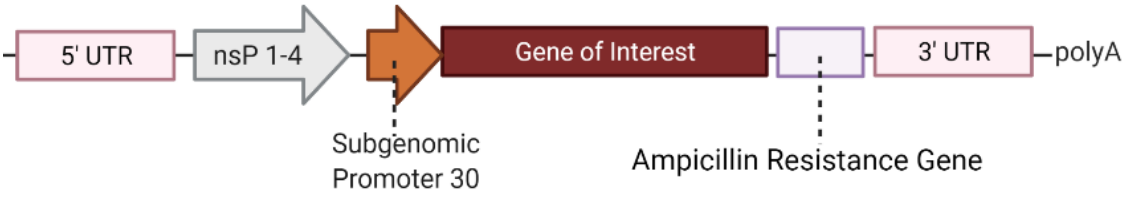

Figure 2. Example RNA replicon vector

From left to right: RNA replicon vector with 5' untranslated region, nsP 1-4, subgenomic promoter, a gene of interest, ampicillin resistance gene, 3' untranslated region, and poly adenine tail. Made with Biorender.

An alphavirus RNA replicon vector is made up of five main parts depicted in Figure 2: a 5' untranslated region containing an SP6 or T7 (SP6 RNA polymerase promoter and T7 RNA polymerase respectively) promoter, non-structural replicase genes, a subgenomic promoter, foreign gene(s) of interest, and polyadenine (polyA) tail at the 3' untranslated region end (Lundstrom, 2014). The SP6/T7 promoter and nonstructural replicase genes make up what is known as the replicase complex. The SP6 phage promoter is a prokaryotic promoter that is recognized by the SP6 bacteriophage RNA polymerase with high processivity. When used for *in vitro* transcription, the SP6 promoter is capable of driving the sense or antisense transcript depending on the orientation of the gene of interest by catalyzing the formation of RNA from DNA from the 5' to 3' direction (Melton et al., 1984). Another common promoter with characteristics similar to SP6 is the T7 promoter from the T7 bacteriophage. The T7 polymerase is a specialized enzyme that binds to the T7 promoter transcribing for the bacteriophage T7 genome but also has applications to

synthesize RNA off linearized DNA templates with high specificity (Arnaud-Barbe et al., 1998; Rong et al., 1998).

The non-structural replicase genes are essential in initiating transcription and translation of replicon RNA as well as regulating viral replication and assembly, but they are not packaged into a viral particle (Uversky & Longhi, 2011). Alphaviruses contain four non-structural proteins (nsP1, nsP2, nsP3, and nsP4) that are essential for transcription and translation with their independent domain function forming what is called the replicase complex or RNA-dependent RNA polymerase (RDRP) (Blakney et al., 2021). nsP1 is an mRNA capping enzyme that has a guanine-7-methyltransferase and guanylyltransferase (GTase) which directs the methylation and capping of the synthesized viral genomic and subgenomic RNAs to prevent RNA degradation by cellular 5' exonucleases (Abu Bakar & Ng, 2018). nsP2 functions as a helicase domain acting as an RNA triphosphatase important for the first series of the viral RNA capping reactions and as a nucleotide triphosphatase driving RNA helicase activity (Abu Bakar & Ng, 2018; Blakney et al., 2021). Early studies aiming to engineer replicons used puromycin acetyltransferase to select for mutations in nsP2 in Sindbis virus replicons that control for cytopathicity (Frolov et al., 1999). nsP3 consists of three domains: an N-terminal macrodomain with phosphatase activity and nucleic acid binding ability, the alphavirus unique domain, and the C-terminal hypervariable domain (Abu Bakar & Ng, 2018; Blakney et al., 2021). The function of this nsP is not well understood but studies have shown the loss of function of nsP3 leads to low viral pathogenicity making it essential for viral RNA transcription regulation (Blakney et al., 2021; Tuittila et al., 2000). nsP4 functions as an RNA polymerase at the C-terminal end that participates in replicating the genomic RNA off the negative-strand RNA and

transcribing the subgenomic RNA (Abu Bakar & Ng, 2018; Blakney et al., 2021). When designing RNA replicons, it is important to consider various mutants because each non-structural protein plays a role in affecting gene expression.

Downstream of the non-structural proteins in the alphavirus RNA is the subgenomic promoter, which encodes the structural proteins required for assembling new viral particles in the original virus, but which are replaced with genes of interest in therapeutic replicons. The subgenomic promoter is a specialized promoter that is included in a virus for heterologous expression of a gene to initiate protein translation that can greatly enhance the level of protein expression (Kim et al., 2014). RNA replicons can then be *in vitro* transcribed and capped with a polyA tail added at the end of RNA transcription for efficient translation while protecting the RNA molecule from enzymatic degradation (Guhaniyogi & Brewer, 2001). Each part plays a major role in the generation of replicons and will determine how high the level of gene expression will be. The system is flexible and amenable for therapeutic efficacy and immunomodulation and warrants further investigation.

Interleukin-12 and interleukin-18 family biology & synergism

Interleukin-12 family

The interleukin-12 (IL-12) family is made up of a group of heterodimeric cytokines including IL-12, IL-23, IL-27, and IL-35 (Vignali & Kuchroo, 2012). IL-12 was first discovered in 1989 as a natural killer cell-stimulatory factor acting as a pleiotropic cytokine on peripheral blood lymphocytes (Kobayashi et al., 1989). IL-12 is encoded by two genes,

IL-12A (p35 subunit) and *IL-12B* (p40 subunit). When combined via disulfide bonds, these two subunits form the bioactive heterodimer of IL-12 known as IL-12p70 with a molecular weight of 70 kilodaltons (kDa) (Gee et al., 2009).

IL-12 plays a major immunomodulatory role in regulating inflammation, anti-tumor immunity, differentiating naïve T-lymphocytes, innate responses, and controlling the type and duration of the adaptive immune response through the production of IFN-γ (Gazzinelli et al., 1993; Schulz et al., 2009). Specialized immune cells such as antigen-presenting cells (APCs) like dendritic cells, monocytes, macrophages, and B-cells primarily produce IL-12 when activated by Toll-like receptors (TLRs) (Trinchieri, 1998). Upon stimulation by IL-12, signal transducer and activator of transcription 4 (STAT4), a critical transcription factor regulator of inflammation, becomes phosphorylated which interacts and phosphorylates c-Jun activating activator protein-1 (AP-1) for downstream signaling (Nakahira et al., 2002).

Interleukin-18 and the interleukin-1 family

The interleukin-1 (IL-1) family consists of a group of 11 cytokines, including IL-1, IL-18, IL-33, and IL-36, that play a role in regulating innate immunity in response to infection (Dinarello, 2018). Interleukin-18 (IL-18), an 18 kDa pro-inflammatory cytokine encoded by the *IL18* gene is produced in several cell types, such as macrophages (Dinarello, 1999), neuronal cells in the gut (Jarret et al., 2020), Kupffer cells (Seki et al., 2001), and smooth muscle cells (Gerdes et al., 2002). IL-18 was first discovered in 1989 as an "IFN-γ -inducing factor" (IGIF) in the serum of mice who received an intraperitoneal injection of endotoxin (K. Nakamura et al., 1989). The gene encoding for IGIF was later

cloned in 1995 for structural analysis comparing the novel cytokine to others found in the IL-1 family such as IL-1α, IL-1β, and IL-1Rα (K. Nakamura et al., 1989).

The similarities it holds with IL-1 is that it comes in two structural flavors, a 24 kDa precursor, known as pro-IL18, containing a propeptide sequence that requires enzymatic cleavage by caspase-1 (also known as IL-1β converting enzyme, ICE) at an aspartic acid to create the mature bioactive form. This occurs upon inflammasome activation either by stimulation of Toll-like receptors in response to a pathogen-derived activator such as a viral or bacterial infection, leading to the generation of active caspase-1 (Afonina et al., 2015). This causes a cascade effect and the active secretion of IL-18 and also IL-1β which follows the same pathway. Interestingly, IL-1β and IL-18, unlike other cytokines, do not have a signal peptide required for secretion (Okamura et al., 1995).

Conventional mechanism of action of IL-1-family cytokines

NLRP3 inflammasomes (also known as cryopyrin) are multimeric protein complexes assembled in the cytosol upon recognition of pathogen- and danger-associated molecular patterns (PAMPs and DAMPs) via TLRs and NOD-like receptors (NLRs). This leads to a downstream activation signal cascade of the nuclear factor kappa light chain enhancer of activated B-cells (NF-κB) pathway (T. Liu et al., 2017). This initial priming signal leads to the subsequent activation of pro-inflammatory cytokines IL-1β and IL-18 in a caspase-1 dependent manner (Ghiringhelli et al., 2009). Activated caspases are triggered by the activated inflammasome and cleave precursors of IL-1β and IL-18 to become bioactive and to be released from the cytosol.

During this process, gasdermin D activation occurs downstream of inflammasome activation. Gasdermin D has been shown to activate pyroptosis which is required for

bioactive IL-1 and IL-18 release through the formation of the gasdermin pores bypassing the proteolytic cleavage by caspase-1 without the need of a signal peptide unlike traditional secretory proteins (Brough & Rothwell, 2007; He et al., 2015). Pyroptosis is an inflammatory form of programmed cell death through the formation of membrane pores by the innate immune system in response to danger signals and microbial infection (X. Liu et al., 2016). Pyroptosis is a form of immunogenic cell death (ICD) where cell death results in activation of an immunological response. Release of IL-1 and IL-18 through gasdermin pores have been shown to induce potent immunological response via pyroptosis which occurs after the release of the contents within the cell leading to morphological changes and destruction of the pyroptotic cell (Brough & Rothwell, 2007). The release of the contents allows for the distribution of immunogenic molecules that can further be used to enhance an ongoing immunological response against cancer cells as a potential strategy.

The role of the NLRP3 inflammasome and pyroptosis is highly dependent on the environmental context in which it becomes activated. The NLRP3 inflammasome has been implicated in the initiation and propagation of various types of autoimmune diseases such as type I and II diabetes, inflammatory bowel disease (IBD), and multiple sclerosis, suggesting that regulation of this pathway is essential to prevent the onset of disease (Guo et al., 2015). Yet in colitis-associated colorectal cancer, activation of the inflammasome and IL-18 signaling pathways have been mainly protective (Zaki et al., 2010). Moreover, NLRP3 inflammasome activation has been shown to negatively impact NK cell-mediated responses in murine melanoma lung metastasis models by limiting the production of IFN-γ (Chow et al., 2012). Further investigation is required to better understand the mechanisms associated with the secretory mechanisms of IL-18 in a cancer context.

Synergy of Interleukin-12 and Interleukin-18

It has been well established that IL-12 synergizes with IL-18 by acting as a key driver for the production of IFN-γ (Nakahira et al., 2002). Some studies have explored the use of IL-12 and IL-18 together leading to tumor-specific immunity and IFN-γ production as a result of immunomodulation in human T-cells (Choi et al., 2011; Tominaga et al., 2000). However, adverse effects have been linked to IL-12 and IL-18 therapy showing increases in mortality and toxicity in both an IFN-γ-dependent and independent manner. This suggests temporal control of these two cytokines may lead to better long-term responses while reducing the risk of adverse side effects (S. Nakamura et al., 2000). It is not well understood if activating both the IL-12 and IL-18 pathways simultaneously and transiently will lead to immunomodulation that is controllable and adaptive warranting further investigation utilizing RNA replicons.

Scope of Thesis

Transient gene expression is a widely investigated strategy that allows for a brief-expression of genes that can be engineered to improve protein production. Currently, regulation of heterologous transient gene expression *in vitro* and *in vivo* has been accomplished with alphavirus/flavivirus-based RNA replicon vaccines (Geall et al., 2012). Alphavirus/flavivirus-based replicons are self-amplifying DNA or RNA molecules typically packaged in virus-like particles that have the capacity of generating high levels of transient heterologous gene expression in vitro and in vivo. These platforms consist of non-structural proteins (nSPs) for amplification which cannot produce infectious progeny by surpassing host genomic integration unlike DNA-based modalities (Varnavski et al., 2000).

Proof-of-concept studies suggest that self-amplifying RNA replicons can be encapsulated in lipid nanoparticles which fuse with the cellular membrane and deposit cargo inside the cell cytosol to be translated into protein (Geall et al., 2012). *Melo et al*. showed Venezuelan encephalitis equine (VEE) eOD-GT8 replicons (an engineered protein designed to engage B-cell receptors) enabled functional protein production via intramuscular injection. This platform enabled controlled release and immunogenic protection against HIV (Melo et al., 2019). The intramuscular route of administration is highly relevant for vaccine development. However, few *in vitro* models exist to provide insight into the mechanism of uptake and protein expression in muscle.

Li et al. demonstrated that VEE-RNA replicons can be engineered to produce a favorable pharmacokinetic release of interleukin-2 (IL-2), a class of glycoproteins produced by leukocytes, that regulates and modulates immune responses by generating a robust anti-tumor response against murine B16F10 melanoma by *in vitro* transcription (Li et al., 2019). A follow-up study has been conducted using interleukin-12 (IL-12)—and interferon-gamma (IFN-γ) inducing factor known for the primary driver of the development of Th1 responses—using an in-house VEE-replicon backbone to eradicate large established solid tumors and suggesting the potential of this platform for therapeutic efficacy (Li et al., 2020).

Interleukin-18 (IL-18), a pro-inflammatory cytokine also known as IFN-γ inducing factor, encoded by the *IL18* gene is produced in several cell types, such as macrophages and muscle cells. Unlike most cytokines in the IL-1 family, IL-18 and IL-1β lack a signal peptide typically required for extracellular release. Instead, wild type IL-18 begins as a precursor containing a pro-peptide sequence (proIL-18; 1-35 amino acids; cleavage at

aspartic acid position 35) that is typically cleaved—before releasing from the cell—by caspase-1 produced by inflammasome activity in response to inflammation (Afonina et al., 2015). During inflammation, activation of the NLRP3 inflammasome occurs through either Toll-like receptor (TLR) stimulation by pathogen-associated molecular pattern molecules (PAMPs) which activate NF-κB signaling. NF-κB leads to the recruitment of the enzyme caspase-1. Recent studies have also shown cleavage of IL-18 independent of caspase-1 activity by mast cell chymase, a family of serine proteases (Omoto et al., 2006).

ProIL-18 undergoing proteolytic cleavage to form mature IL-18 is well accepted but very few methods highlight IL-18 and its role in ICD and pyroptosis. Therefore, a transient expression system of proIL-18 and mature IL-18 using an RNA replicon system can help mitigate chronic dysregulation of a pathway highly associated with autoimmunity (Boraschi & Dinarello, 2006). This method will also allow for an investigation into pyroptosis by overloading cells with a fully functional secretory cytokine that becomes active upon cell death to further enhance an immunological response.

The hypothesis proposed in this thesis is that mature IL-18 can be bioactive without a signal peptide using a dual self-amplifying RNA replicon construct with IL-12 to induce pyroptosis and increase the production of IFN-γ. The first half of the work focuses on the design, fabrication, and validation of various IL-18 replicons. The second goal of this work is to demonstrate whether conventional synergy can be obtained through a dual-format replicon to examine the mechanism of secretion and biological activity. The data generated from *in vitro* experiments will provide evidence to support how IL-12 and IL-18 can be produced in a dual RNA replicon format while also examining mechanisms associated with inflammation and pyroptosis. These aims can be modified to impact research devoted to

enhancing the production of protein biologics and the utilization of already existing cellular machinery to combat cancer.

Outline of the Thesis

The experimental work carried out to fulfill the objectives discussed in the introductory chapter is presented in Chapters II, III, IV, and V of this thesis. Chapter II details the preparation of the materials as well as cell culture *in vitro* experiments and analytical methods are described here. Chapter III discusses the results from the *in vitro* validation experiments. This follows into Chapter IV describing the results from the synergistic studies done uniting the results discussed in Chapter III. The thesis concludes in Chapter V with a summary of the conclusions gathered in this work and a discussion on future directions and outlooks.

Chapter II.

Materials and Methods

Constructs, in vitro transcription, capping/methylating replicon RNAs

An overview of the RNA replicon synthesis workflow is denoted in Figure 3. Plasmid constructs were designed using SnapGene. Murine IL-18 sequence (Accession: D49949.1, Mus musculus IGIF mRNA for interferon-gamma inducing factor) was obtained from previously published work and verified on the National Center for Biotechnology Information database ("Database Resources of the National Center for Biotechnology Information," 2016; Okamura et al., 1995). Murine scIL-12 and scIL-12 moues serum albumin (MSA) sequences were obtained from previously published work (Li et al., 2020; Momin et al., 2019). Standard recombinant DNA techniques for plasmid construction were used for all plasmid constructions using a Gibson Assembly Cloning Kit and finished plasmids were sent out for DNA sequencing for validation (New England Biolabs, cat. no. E5510S; Figure 3A, 3B).

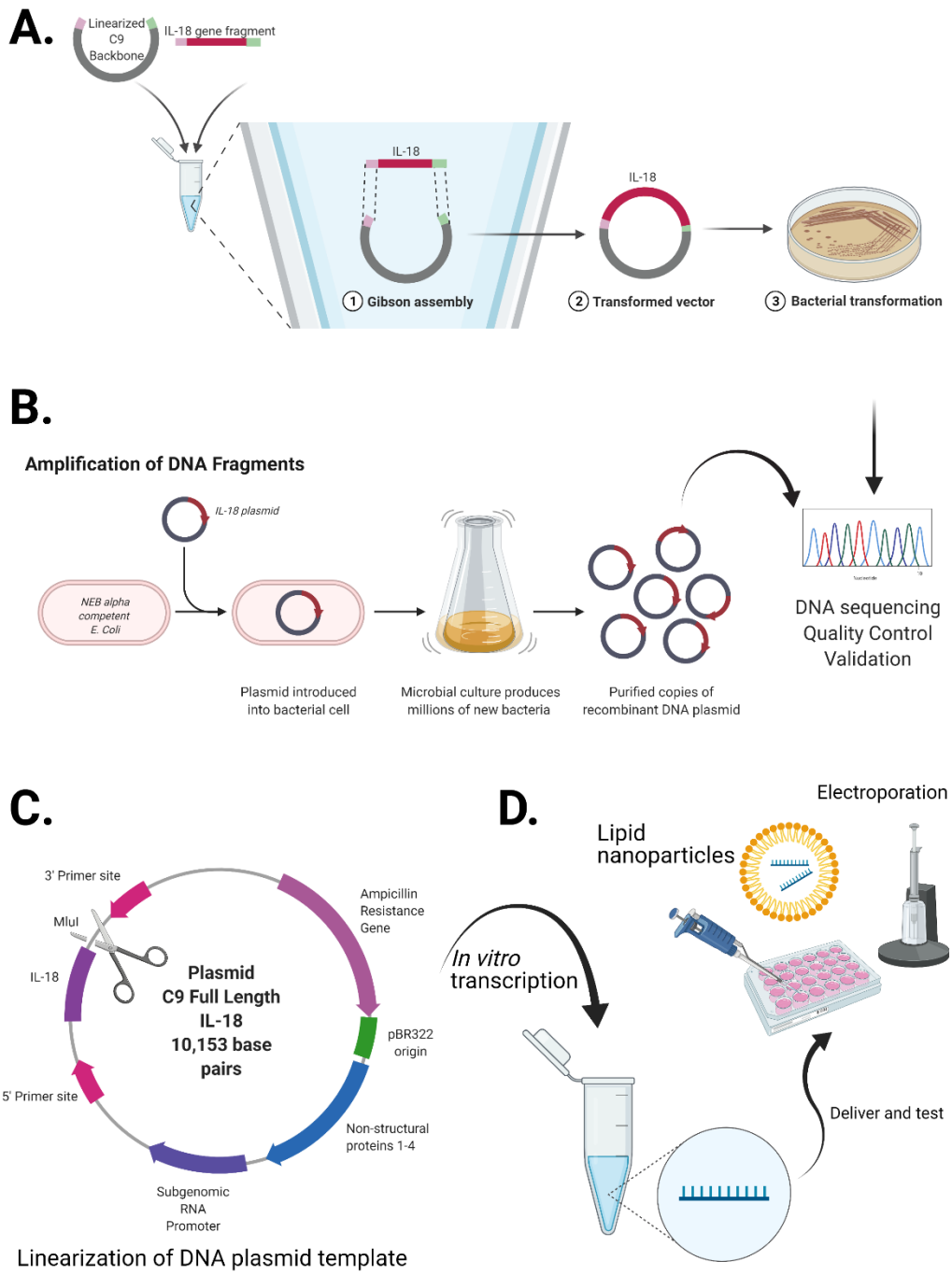

Figure 3. Overview of RNA replicon synthesis workflow.

***A**. Gibson Assembly workflow. **B**. Amplification of plasmid, selection, and DNA sequencing validation of sequence. **C**. Linearization of DNA plasmid template. **D**. In vitro transcription of RNA replicon followed by a downstream application for in vitro validation. This illustration was created with BioRender.com*

VEE (denoted as C9 from hereon) replicon plasmid DNA was prepared based on constructs previously described (Li et al., 2019). All constructs are on the C9 RNA replicon backbone. mCherry, an RNA replicon encoding for a red fluorescent protein, was cloned after the subgenomic promoter to generate reporter constructs as previously described (Li et al., 2019). scIL-12-MSA fusion payload gene was cloned with sequences as previously described (Momin et al., 2019). The Full-Length IL-18 sequence consists of the murine IL-18 sequence including the precursor polypeptide. Active IL-18 sequence contains no precursor polypeptide. tsPa (also commonly abbreviated tPa or tPa-SP) refers to a human tissue plasminogen activator sequence replacing the precursor polypeptide sequence on IL-18 with an 81% homology to mouse tsPa (Rickles et al., 1988). These sequences are denoted as tsPa IL-18. Single chain IL-12 is denoted as scIL-12 that used previously (Li et al., 2020). Dual constructs were designed to combine scIL-12 and the three different IL-18 formats described above. Between each sequence is a P2A self-cleaving peptide to allow for ribosomal skipping during translation of a protein in a cell (Z. Liu et al., 2017). Examples of a gene of interest are depicted in Figure 4. The following plasmid vectors were amplified and cloned and protein sequences are described in Figure 4 and Table 1 below:

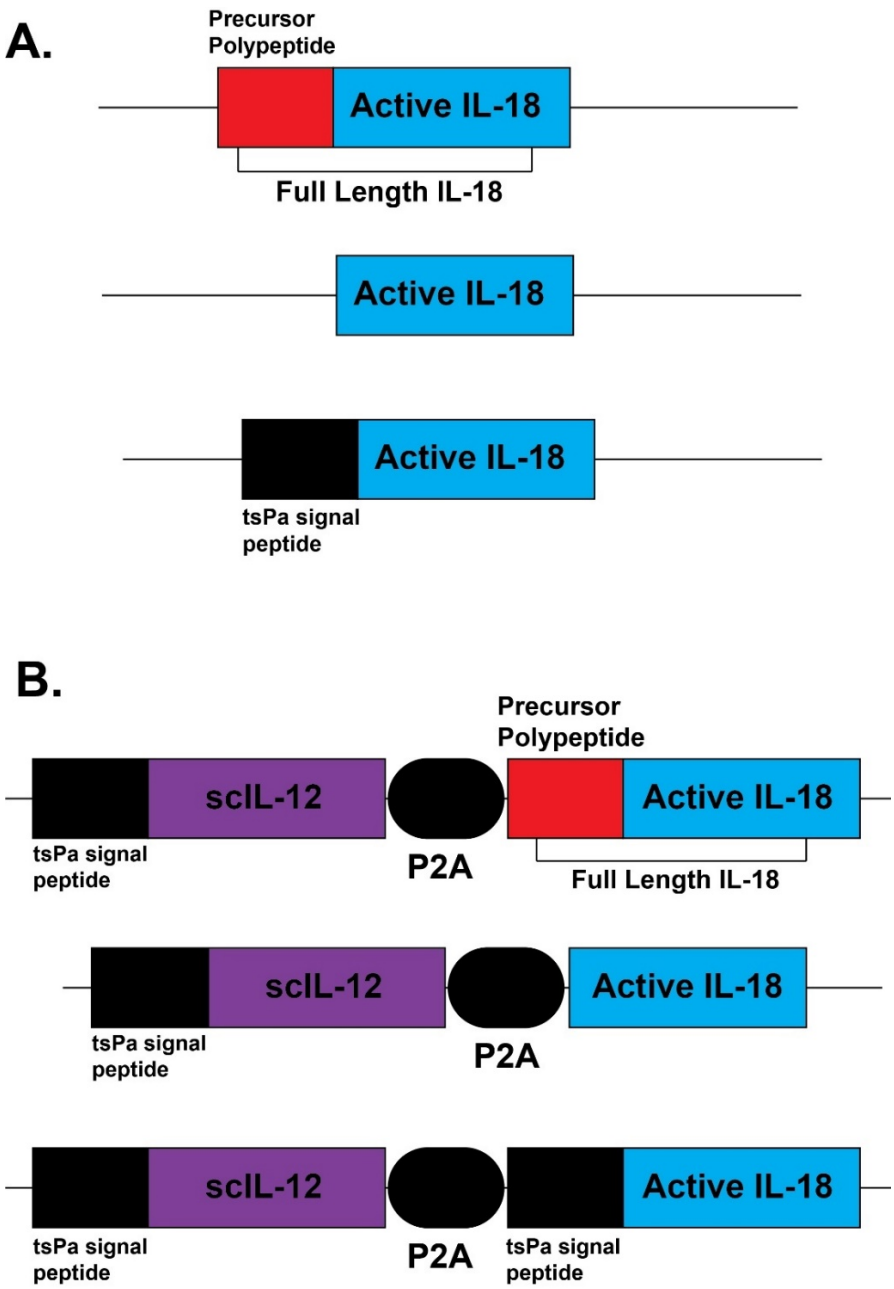

Figure 4. Schematic of single replicon and dual constructs.

A. From top to bottom: Full-Length IL-18, Active IL-18, and tsPa IL-18. B. From top to bottom: scIL12 and Full-Length IL-18, scIL-12 and Active IL-18, and scIL-12 and tsPa IL-18.

Table Format	Table Legend	Description
Protein Name (N to C terminus composition)	Red	Precursor polypeptide
	Blue	IL-18
	Purple	IL-12
	Green	Mouse Serum Albumin
	Orange	mCherry
N to C terminus amino acid sequence	Black	Linker
	Black	tsPa signal peptide
	Green	P2A self-cleaving peptide

Name	Protein Sequence
Full-Length IL-18	MAAMSEDSCVNFKEMMFIDNTLYFIPEENGDLESDNFGRLHCTTAVIRNINDQVLFVDKRQPVFEDMTDIDQSASEPQTRLIIYMYKDSEVRGLAVTLSVKDSKMSTLSCKNKIISFEEMDPPENIDDIQSDLIFFQKRVPGHNKMEFESSLYEGHFLACQKEDDAFKLILKKKDENGDKSVMFTLTNLHQS
Active IL-18	NFGRLHCTTAVIRNINDQVLFVDKRQPVFEDMTDIDQSASEPQTRLIIYMYKDSEVRGLAVTLSVKDSKMSTLSCKNKIISFEEMDPPENIDDIQSDLIFFQKRVPGHNKMEFESSLYEGHFLACQKEDDAFKLILKKKDENGDKSVMFTLTNLHQS
tsPa IL-18	ATGGATGCAATGAAGCGGGGGCTCTGCTGTGTGTTGCTGCTGTGCGGCGCCGTCTTCGTCTCTCCATCCNFGRLHCTTAVIRNINDQVLFVDKRQPVFEDMTDIDQSASEPQTRLIIYMYKDSEVRGLAVTLSVKDSKMSTLSCKNKIISFEEMDPPENIDDIQSDLIFFQKRVPGHNKMEFESSLYEGHFLACQKEDDAFKLILKKKDENGDKSVMFTLTNLHQS

scIL-12 and Full-Length IL-18	MWELEKDVYVVEVDWTPDAPGETVNLTCDTPEEDDITWTSDQR HGVIGSGKTLTITVKEFLDAGQYTCHKGGETLSHSHLLLHKKENG IWSTEILKNFKNKTFLKCEAPNYSGRFTCSWLVQRNMDLKFNIKS SSSSPDSRAVTCGMASLSAEKVTLDQRDYEKYSVSCQEDVTCPTA EETLPIELALEARQQNKYENYSTSFFIRDIIKPDPPKNLQMKPLKNS QVEVSWEYPDSWSTPHSYFSLKFFVRIQRKKEKMKETEEGCNQK GAFLVEKTSTEVQCKGGNVCVQAQDRYYNSSCSKWACVPCRVR SGGSGGGSGGGSGGGSRVIPVSGPARCLSQSRNLLKTTDDMVKTA REKLKHYSCTAEDIDHEDITRDQTSTLKTCLPLELHKNESCLATRE TSSTTRGSCLPPQKTSLMMTLCLGSIYEDLKMYQTEFQAINAALQ NHNHQQIILDKGMLVAIDELMQSLNHNGETLRQKPPVGEADPYR VKMKLCILLHAFSTRVVTINRVMGYLSSAGGAAGCGGGGCAACT AATTTCTCCTTGCTTAAGCAAGCAGGGGACGTCGAGGAAAATC CGGGTCCTMAAMSEDSCVNFKEMMFIDNTLYFIPEENGDLESDNF GRLHCTTAVIRNINDQVLFVDKRQPVFEDMTDIDQSASEPQTRLII YMYKDSEVRGLAVTLSVKDSKMSTLSCKNKIISFEEMDPPENIDDI QSDLIFFQKRVPGHNKMEFESSLYEGHFLACQKEDDAFKLILKKK DENGDKSVMFTLTNLHQS
scIL-12 and Active IL-18	MWELEKDVYVVEVDWTPDAPGETVNLTCDTPEEDDITWTSDQR HGVIGSGKTLTITVKEFLDAGQYTCHKGGETLSHSHLLLHKKENG IWSTEILKNFKNKTFLKCEAPNYSGRFTCSWLVQRNMDLKFNIKS SSSSPDSRAVTCGMASLSAEKVTLDQRDYEKYSVSCQEDVTCPTA EETLPIELALEARQQNKYENYSTSFFIRDIIKPDPPKNLQMKPLKNS QVEVSWEYPDSWSTPHSYFSLKFFVRIQRKKEKMKETEEGCNQK GAFLVEKTSTEVQCKGGNVCVQAQDRYYNSSCSKWACVPCRVR SGGSGGGSGGGSGGGSRVIPVSGPARCLSQSRNLLKTTDDMVKTA REKLKHYSCTAEDIDHEDITRDQTSTLKTCLPLELHKNESCLATRE TSSTTRGSCLPPQKTSLMMTLCLGSIYEDLKMYQTEFQAINAALQ NHNHQQIILDKGMLVAIDELMQSLNHNGETLRQKPPVGEADPYR VKMKLCILLHAFSTRVVTINRVMGYLSSAGGAAGCGGGGCAACT AATTTCTCCTTGCTTAAGCAAGCAGGGGACGTCGAGGAAAATC CGGGTCCTNFGRLHCTTAVIRNINDQVLFVDKRQPVFEDMTDIDQ SASEPQTRLIIYMYKDSEVRGLAVTLSVKDSKMSTLSCKNKIISFEE MDPPENIDDIQSDLIFFQKRVPGHNKMEFESSLYEGHFLACQKEDD AFKLILKKKDENGDKSVMFTLTNLHQS

scIL-12 and tsPa IL-18

MWELEKDVYVVEVDWTPDAPGETVNLTCDTPEEDDITWTSDQR
HGVIGSGKTLTITVKEFLDAGQYTCHKGGETLSHSHLLLHKKENG
IWSTEILKNFKNKTFLKCEAPNYSGRFTCSWLVQRNMDLKFNIKS
SSSSPDSRAVTCGMASLSAEKVTLDQRDYEKYSVSCQEDVTCPTA
EETLPIELALEARQQNKYENYSTSFFIRDIIKPDPPKNLQMKPLKNS
QVEVSWEYPDSWSTPHSYFSLKFFVRIQRKKEKMKETEEGCNQK
GAFLVEKTSTEVQCKGGNVCVQAQDRYYNSSCSKWACVPCRVR
SGGSGGGSGGGSGGGSRVIPVSGPARCLSQSRNLLKTTDDMVKTA
REKLKHYSCTAEDIDHEDITRDQTSTLKTCLPLELHKNESCLATRE
TSSTTRGSCLPPQKTSLMMTLCLGSIYEDLKMYQTEFQAINAALQ
NHNHQQIILDKGMLVAIDELMQSLNHNGETLRQKPPVGEADPYR
VKMKLCILLHAFSTRVVTINRVMGYLSSAGGAAGCGGGGCAACT
AATTTCTCCTTGCTTAAGCAAGCAGGGGACGTCGAGGAAAATC
CGGGTCCTATGGATGCAATGAAGCGGGGGCTCTGCTGTGTGTT
GCTGCTGTGCGGCGCCGTCTTCGTCTCTCCATCCNFGRLHCTTA
VIRNINDQVLFVDKRQPVFEDMTDIDQSASEPQTRLIIYMYKDSEV
RGLAVTLSVKDSKMSTLSCKNKIISFEEMDPPENIDDIQSDLIFFQK
RVPGHNKMEFESSLYEGHFLACQKEDDAFKLILKKKDENGDKSV
MFTLTNLHQS

scIL-12 MSA

MWELEKDVYVVEVDWTPDAPGETVNLTCDTPEEDDITWTSDQRHG
VIGSGKTLTITVKEFLDAGQYTCHKGGETLSHSHLLLHKKENGIWSTE
ILKNFKNKTFLKCEAPNYSGRFTCSWLVQRNMDLKFNIKSSSSSPDSR
AVTCGMASLSAEKVTLDQRDYEKYSVSCQEDVTCPTAEETLPIELAL
EARQQNKYENYSTSFFIRDIIKPDPPKNLQMKPLKNSQVEVSWEYPDS
WSTPHSYFSLKFFVRIQRKKEKMKETEEGCNQKGAFLVEKTSTEVQC
KGGNVCVQAQDRYYNSSCSKWACVPCRVRSGGSGGGSGGGSGGGS
RVIPVSGPARCLSQSRNLLKTTDDMVKTAREKLKHYSCTAEDIDHEDI
TRDQTSTLKTCLPLELHKNESCLATRETSSTTRGSCLPPQKTSLMMTL
CLGSIYEDLKMYQTEFQAINAALQNHNHQQIILDKGMLVAIDELMQS
LNHNGETLRQKPPVGEADPYRVKMKLCILLHAFSTRVVTINRVMGY
LSSAGSGGGSEAHKSEIAHRYNDLGEQHFKGLVLIAFSQYLQKCSYD
EHAKLVQEVTDFAKTCVADESAANCDKSLHTLFGDKLCAIPNLREN
YGELADCCTKQEPERNECFLQHKDDNPSLPPFERPEAEAMCTSFKEN
PTTFMGHYLHEVARRHPYFYAPELLYYAEQYNEILTQCCAEADKESC
LTPKLDGVKEKALVSSVRQRMKCSSMQKFGERAFKAWAVARLSQT
FPNADFAEITKLATDLTKVNKECCHGDLLECADDRAELAKYMCENQ
ATISSKLQTCCDKPLLKKAHCLSEVEHDTMPADLPAIAADFVEDQEV
CKNYAEAKDVFLGTFLYEYSRRHPDYSVSLLLRLAKKYEATLEKCC
AEANPPACYGTVLAEFQPLVEEPKNLVKTNCDLYEKLGEYGFQNAIL
VRYTQKAPQVSTPTLVEAARNLGRVGTKCCTLPEDQRLPCVEDYLSA
ILNRVCLLHEKTPVSEHVTKCCSGSLVERRPCFSALTVDETYVPKEFK
AETFTFHSDICTLPEKEKQIKKQTALAELVKHKPKATAEQLKTVMDD
FAQFLDTCCKAADKDTCFSTEGPNLVTRCKDALA

mCherry	MVSKGEEDNMAIIKEFMRFKVHMEGSVNGH EFEIEGEGEG RPYEGT QTAKLKVTKGGPLPFAWDILSPQFMYGSKAYVKH PADIPDYLKLSFP EGFKWERVMNFEDGGVVTVTQDSSLQDGEFIYKVKLR GTNFPSDGP VMQKKTMGWEASSERMYPEDGALKGEIKQRLKLKDGGHYDAEVKT TYKAKKPVQLPGAYNVNIKLDITSHNEDYTIVEQYE RAEGRHSTGG MDELYK
C9 Backbone Primers Forward/Reverse	AGAGGCAGCCTGTTTTGAA / GGGGATCCATCTCCTCAAAT
Dual replicon internal #1 primer	GGTGCAGCGAAACATGGATC
Dual replicon internal #2 primer	TTGCTCTAAGTGGGCCTGTG

Table 1. List of RNA replicon protein sequences and primer sequences

This table lists all used RNA replicon protein sequences and primer sequences with table legend

These plasmids were cloned after the subgenomic promoter to generate experimental single and dual replicon constructs. Protein sequences of all constructs can be found in Table 1 in the appendix.

Linearized DNA templates were generated by cutting with MluI-HF in CutSmart buffer per manufacturer's instruction (New England Biolabs, cat. no. R3198S; Figure 3C). Replicon RNAs were *in vitro* transcribed (IVT) from the templates of linearized C9 DNA plasmids constructs using the MEGAscript T7 transcription kit (Thermo Fisher Scientific) following the manufacturer's instructions. The replicon RNAs were capped and methylated using the ScriptCap m7G Capping System and ScriptCap 2'-O-methyltransferase kit

(CellScript) according to the manufacturer's instructions (Figure 3D). RNA purity was assessed on a 1% formaldehyde agarose gel electrophoresis post IVT and post polyA capping (Figure 5).

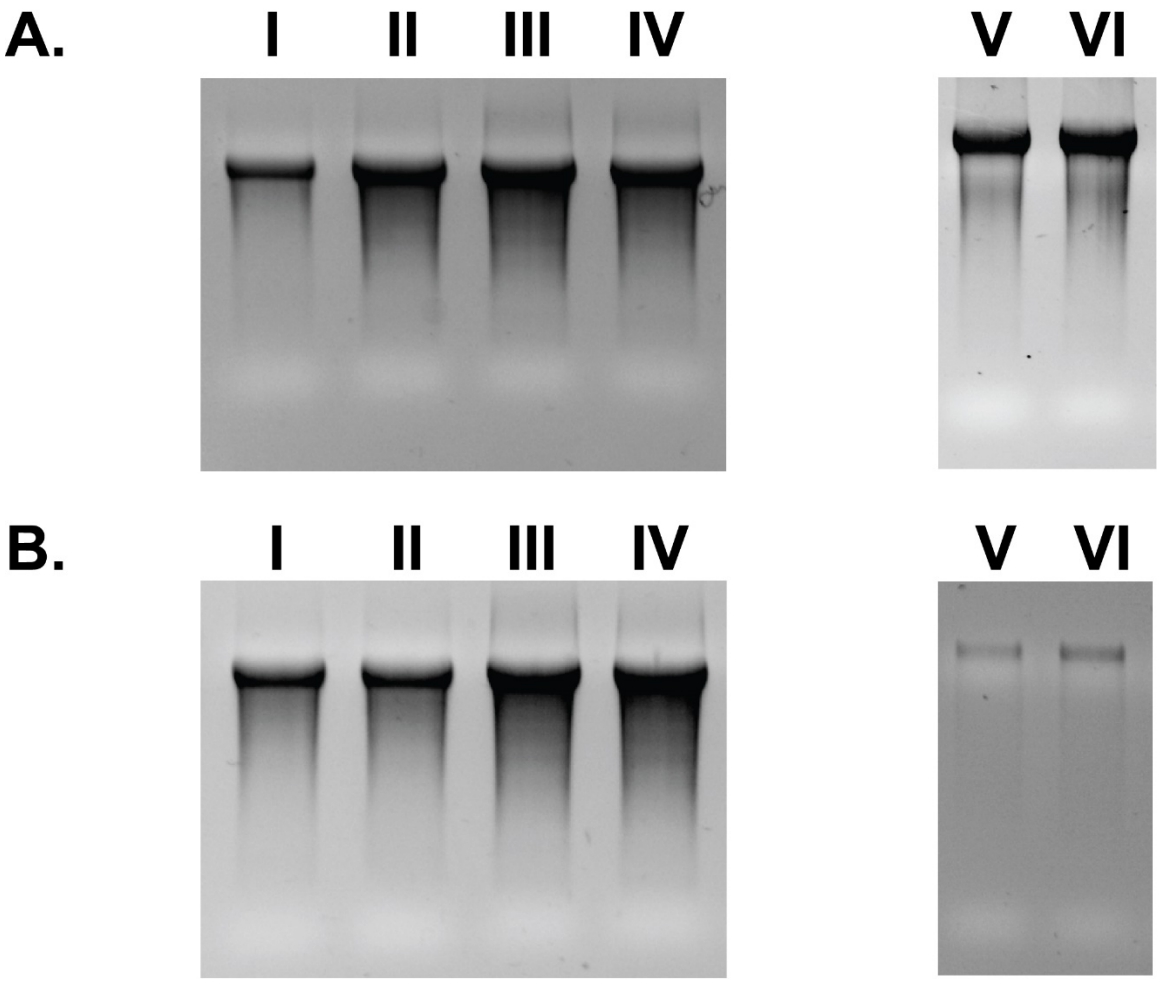

Figure 5. Quality control by gel electrophoresis of RNA replicons for RNA integrity.

A I-VI. *1% formaldehyde agarose gel electrophoresis of uncapped RNA replicons from left to right:* ***I*** *- C9 Full-Length IL18,* ***II*** *- C9 Active IL18,* ***III*** *- C9 tsPa IL18,* ***IV*** *- C9 scIL12, and Active IL18,* ***V*** *- C9 scIL12 and Full-Length IL18, and* ***VI*** *- C9 scIL12 and tsPa IL18.* ***B I-VI.*** *1% formaldehyde agarose gel electrophoresis of capped RNA replicons from left to right of same constructs as* ***Figure 5A I-VI****.*

Concentration was quantified using a NanoDrop microvolume UV-Vis spectrophotometer (Thermo Fisher). All RNA replicon constructs were stored in -80°C.

Delivery and encapsulation of IL-18 and scIL12/IL-18 RNA replicons in lipid nanoparticles

For delivery of 1 ug of each replicon RNA, Lipofectamine MessengerMAX nanoparticles were used following the manufacturer's instructions (Thermo Scientific). In brief, $0.5x10^5$ cells are seeded the day before to allow for cells to adhere. All lipid transfection experiments were carried out on 24 well tissue culture-treated plates (Corning cat. no. 353047). Lipiofectamine nanoparticles were formulated in Opti-MEM I reduced serum medium (Thermo Fisher, cat. no. 31985062). Lipofectamine was mixed and incubated in Opti-MEM I for 10 minutes at room temperature. RNA replicons were diluted and scaled accordingly based on study design to deliver 1 μg of RNA replicon per well in 500 μL total medium. The hydrodynamic size of lipofectamine nanoparticles was measured using dynamic light scattering (Malvern). Both lipofectamine mixture and diluted RNA replicons were mixed and incubated for 5 minutes at room temperature before adding dropwise to each well. Cells were transfected for 4 hours in 500 μL of complete media containing no antibiotics followed by a media change at the end of the transfection and allowed to recover for 24 hours or more depending on experimental design.

Electroporation in vitro validation assays

In vitro validation via electroporation transfection experiments were carried out in 6 well tissue culture-treated plates (Corning cat. no. 353046) using electroporation of 1 ug of RNA per 20,000 C2C12 cells in 100 μl of R buffer using a NEON transfection kit

(Thermo Fisher Scientific) at 1,650 volts, 10 ms, and three pulses. For RAW264.7 cells, electroporation of 1 ug of RNA per 20,000 RAW264.7 cells in 100 µl of R buffer using the NEON transfection kit as described above at 1,680 volts, 20-millisecond pulse width, one pulse. Electroporated cells were incubated in complete media for 24 up to 48 hours post-transfection and supernatant/cell lysate was collected. Frozen samples were kept at -80°C.

Supernatants were transferred into 96 well 0.5 mL V-bottom polypropylene matrix tube racks with lids (Thermo Fisher Scientific, cat. no. 3725TS) and frozen down at -80°C. Cell lysates were lysed with NP-40 buffer made with 150 mM sodium chloride, 1.0% NP-40, 50 mM Tris pH 8.0 with 1x Halt Protease Inhibitor Cocktail (Thermo Fisher Scientific, cat. no. 87786) for 30 minutes gently rocking at 4°C before centrifuged on a swinging bucket rotor at max speed to remove debris. Individual vials were removed from the rack for thawing to minimize freeze-thaw cycles. The thawing of samples was kept to a minimum of 2 times per sample.

Cell lines and animals

Cell lines C2C12 (ATCC CRL-1772), RAW264.7 (TIB-71), B16F10 (ATCC CRL-6475), and HEK Blue IL-18 (Invivogen) were cultured following vendor instructions. Frozen cells and culture supernatants were sent out to be tested for mycoplasma at the Koch Institute Swanson Biotechnology Center before experimentation. Female C57BL/6 (The Jackson Laboratory stock no. 000664) mice at 6-8 weeks of age were purchased and maintained at the animal facility at the Massachusetts Institute of Technology. All animal procedures were carried out following federal, state, and local guidelines under an institutional animal care and use committee-approved protocol by the Committee of Animal Care at MIT.

Antibodies, staining, and FACs analysis

Antibodies against mouse CD45 PerCP-Cy5.5 (clone 30-F11), CD3ε BV605 (clone 145-2C11), NK1.1 BV785 (clone PK136), CD11b APC-Cy7 (clone M1/70), CD19 BV421 (clone 6D5), CD218α/IL-18R APC (clone A17071D), IL12p40 PE-Cy7 (clone C15.6), and IFN-γ BV711 (clone XMG1.2) were obtained from Biolegend. Antibodies against mouse CD4 BUV395 (clone GK1.5) and CD8 BUV737 (clone 53-6.7) were obtained from BD Biosciences. Antibody against purified mouse IL-18 (clone YIGIF74-1G7) was obtained from InVivoMab and labeled with an Alexa Fluor 488 Microscale Protein Labeling kit from Thermo Fisher Scientific. All antibodies except IL12p40, IFN-γ, and IL-18 were diluted at 1:200. IL12p40, IFN-γ, and IL-18 antibodies were diluted at 1:75. The live/dead Aqua dye (cat. no. L34966) was from Thermo Fisher Scientific diluted at 1:1000. TruStain FcX mouse CD16/CD32 block (clone 93) was obtained from Biolegend and diluted at 1:1000. Cell staining buffer (cat. no. 420201) was obtained from Biolegend. Precision counting beads were used in some studies to obtain absolute cell counts following the manufacturer's protocol (Biolegend).

All washes and spin speeds were 1500 rpm for 5 minutes at 4°C. Cells washes were done by adding 100 µL of either cell staining buffer or Perm/Wash buffer between each incubation. After harvesting cells into 96 well U-bottom or V-bottom plates (Corning cat. no. 3799; Corning cat. no. 3894), cells were washed once with 1x PBS (Corning cat. no. 21-040-CV) before adding 100 µL of live dead Aqua diluted in PBS to samples and control for 15 minutes in the dark at 4°C and then washed. TruStain FcX was diluted in cell staining buffer and added for 10 minutes and washed. Extracellular markers were stained for 15 minutes in the dark at 4°C and washed. Cells are fixed using a 1x CytoFix Fix/Perm kit

(BD Biosciences, cat. no. 554714) for 20 minutes and washed using the provided 10x Perm/Wash buffer diluted to 1x using distilled water. Intracellular markers were diluted in 1x Perm/Wash buffer and stained for 45 minutes before being washed with 1x Perm/Wash. Fixed cells were resuspended in 210 µL of cell staining buffer to account for dead volume in the needle when running on the flow cytometry analyzer (FACS).

Stained samples were analyzed using a FACS analyzer (LSR-II Fortessa) from BD Biosciences. All flow cytometry data were analyzed using FlowJo software (FlowJo LLC).

Splenocyte harvest for *in vitro* cytokine stim assays

Spleens from euthanized 6-8 week old female naïve C57BL/6 mice were harvested. The single-cell suspensions were made by smashing harvested spleens into a 70 µm nylon strainer. Red blood cells were lysed using ACK lysis buffer (Thermo Fisher Scientific), quenched using Roswell Park Memorial Institute 1640 medium (Fisher Scientific) supplemented with 10% FBS, and pelleted down by centrifugation at 1500 rpm for 5 minutes at 4°C. Spleens were filtered again on another 70 µm nylon strainer, counted on a Countess II (Thermo Fisher), and kept on ice before seeded into wells for *in vitro* assays.

Samples collected for flow cytometry analysis were incubated with 1x brefeldin A (Biolegend, cat. no. 420601) for 4 hours. For IFN-γ staining, controls were made in triplicate of brefeldin A only, PMA/ionomycin only (Biolegend, cat. no. 423301), and brefeldin A + PMA/ionomycin. PMA/ionomycin + brefeldin A was incubated for 2 hours each so all samples were incubated for a total of 4 hours at 37°C.

IFN-γ production assay

50,000 B16F10 cells were seeded in 24 well TC treated plates one day prior and transfected with replicon RNA once cells have adhered to the plate overnight as described previously. After 24 hours post-transfection, splenocytes were harvested from naïve C57BL/6 female mice and processed as described previously. Splenocytes were counted as previously described and pooled before staining with Cell Trace Violet for tracking by flow cytometry per manufacturer's instruction (Thermo Fisher, cat. no. C34557). 50,000 splenocytes were seeded into each well for an effector to target ratio of 1:1. The supernatant was collected at 24 hours post splenocyte addition. Samples were frozen down and stored at -80°C for ELISA analysis.

Cytokine stimulation of naïve splenocytes

Two spleens were harvested, processed, and 100,000 total splenocytes were seeded into a 96 U-bottom plate in complete media consisting of RPMI, 10% FBS, 0.0005% β-ME, 1% sodium pyruvate, and 1% penicillin/streptomycin. Cells were then either spiked with recombinant IL-2, recombinant IL-12 (rIL-12), scIL-12 (synthesized in-house), or recombinant IL-18 at two known concentrations except for IL-2. Recombinant IL-2, IL-12, and IL-18 were obtained from Biolegend (cat. no. 575406, 577002, and 767002).

- IL-2 final concentration: 5 ng/mL
- IL-12 final concentration: 0.1 ng/mL (low dose) or 1 ng/mL (high dose)
- scIL-12 final concentration: 0.1 ng/mL (low dose) or 1 ng/mL (high dose)
- IL-18 final concentration: 10 ng/mL (low dose) or 30 ng/mL (high dose)

Cells were then incubated overnight for 24 hours before supernatant was collected for an IFN-γ ELISA followed by intracellular staining for flow cytometry.

ELISA analysis

Levels of IL-18, IL-12, and IFN-γ in the supernatant and cell lysate were measured by ELISA kits from MBL International (cat. no. 7625) and R&D Systems DuoSet ELISA and Quantikine ELISA kits (cat. no. DY419, IL12p70; cat. no. MIF00, IFN-γ) following manufacturer's instruction.

HEK Blue IL-18 SEAP Quantification Assay

HEK Blue IL-18 SEAP colorimetric assays were conducted using QUANTI Blue solution that detects alkaline phosphatase activity in a biological sample per the manufacturer's protocol (InvivoGen). HEK Blue IL-18 cells were transfected with 1 μg of IL-18 RNA replicons for 4 hours followed by 24 hours of recovery in complete media. 100-200 μL of cell supernatants were then collected and spun down at 1500 rpm for 5 minutes at 4°C. The assay was run on a 96 well flat bottom plate. 180 μL of QUANTI Blue solution was added to each sample well and spiked with 20 μL of cell supernatant sample. The assay plate was then incubated for 1 hour before reading on a Tecan 200 Pro microplate reader at a 655 nm excitation wavelength.

Statistics and reproducibility

Results are presented as mean ± standard deviation of the mean. Data were statistically analyzed by one-way or two-way ANOVA using GraphPad PRISM. The sample sizes for *in vitro* analysis were three (technical triplicates) per condition. Standard curves were interpolated using GraphPad PRISM (Version 9.0.2) for ELISA analysis.

Chapter III.

Design, fabrication, and validation of IL-18 replicons

Introduction

In this chapter, the design, fabrication, and validation of RNA replicons discussed in Chapter I is presented here. The objective of this work was to validate the synthesis of IL-18 RNA replicons and demonstrate RNA-produced bioactive proteins with or without a signal peptide when delivered into cells *in vitro*. C2C12 murine myoblast and RAW264.7 murine macrophage cells were chosen as model cell lines for validation experiments.

However, electroporation is only one method of delivering RNA replicons into cells and an alternative relevant for *in vivo* delivery was also tested by encapsulating RNA replicons in lipid nanoparticles. B16F10 was chosen as the experimental workhorse model alongside HEK Blue IL-18, an engineered human embryonic kidney reporter cell line able to detect murine and human IL-18. Experiments in this chapter support the hypothesis that IL-18 RNA replicons can produce bioactive IL-18 without a signal peptide and are further expanded in Chapter IV.

Results

IL-18 RNA replicons delivered via electroporation to C2C12 and RAW264.7 can be quantified in the supernatant and cell lysate by ELISA

IL-18-encoding RNA replicons were designed and fabricated using the Gibson Assembly and IVT as previously described in Chapter II Materials and Methods (Figure 3). To ensure proper translation, RNA replicons need to be of the highest quality. This was validated by running a 1% formaldehyde gel electrophoresis post IVT (Figure 4A) and after capping the RNA replicon with the polyA tail (Figure 4B) to ensure no shadow or extraneous band contaminated the sample during the synthesis.

The different types of constructs designed were briefly discussed in Chapter II Materials and Methods (Table 1 and Figure 4). In brief, a total of six different constructs were designed and fabricated along with control RNA replicons (i.e. scIL-12 MSA and mCherry) based on previously published sequences (Li et al., 2020; Momin et al., 2019, Table 2). mCherry RNA replicons groups were run to confirm transfection efficiency and confirmation of the selected transfection protocol used across experiments. scIL-12 MSA was used as a positive control for IL-12 production and secretion.

Construct Name	Description
Full-Length IL-18	native precursor polypeptide containing murine IL-18
Active IL-18	lacks precursor polypeptide murine IL-18
tsPa IL-18	human tissue plasminogen signal peptide (replaced precursor polypeptide) murine IL-18
scIL-12 and Full-Length IL-18	single-chain IL-12 dual construct with Full-Length IL-18
scIL-12 and Active IL-18	single-chain IL-12 dual construct with murine IL-18 lacking precursor polypeptide
scIL-12 and tsPa IL-18	single-chain IL-12 dual construct with human tissue plasminogen signal peptide (replaced precursor polypeptide) murine IL-18

scIL-12 MSA	single-chain IL-12 fused to mouse serum albumin
mCherry	red fluorescent protein

Table 2. Construct summary with a description of each construct

Description of all RNA replicon constructs fabricated and designed with a detailed explanation of modifications.

C2C12 myoblasts and RAW264.7 macrophages were electroporated with 1 μg of RNA replicon to validate the production of IL-18. Supernatants and cell lysates had a detectable transient expression of IL-18 by ELISA. In C2C12 myoblasts, Full-Length IL-18 and Active IL-18 showed no difference to untreated or electroporated control at 24 or 48 hours in the cell lysate. However, tsPa-IL-18 showed an average of 745.3 pg/mL of IL-18 at 24 hours post-transfection, which continued to rise at 48 hours up to an average of 1,153.6 pg/mL of IL-18 in the cell lysate compared to untreated control ($p<0.0001$) (Figure 6A). Given the results from the previous experiment, a time course was run to quantify tsPa IL-18 in the supernatant to confirm transient gene expression. The supernatant showed a similar increase profile averaging 1,131.6 pg/mL at 24 hours followed by a peak of 1,270.19 pgmL at 48 hours compared to untreated control ($p<0.0001$). The amount of IL-18 began to drop 72 and almost half at 96 hours (Figure 6B).

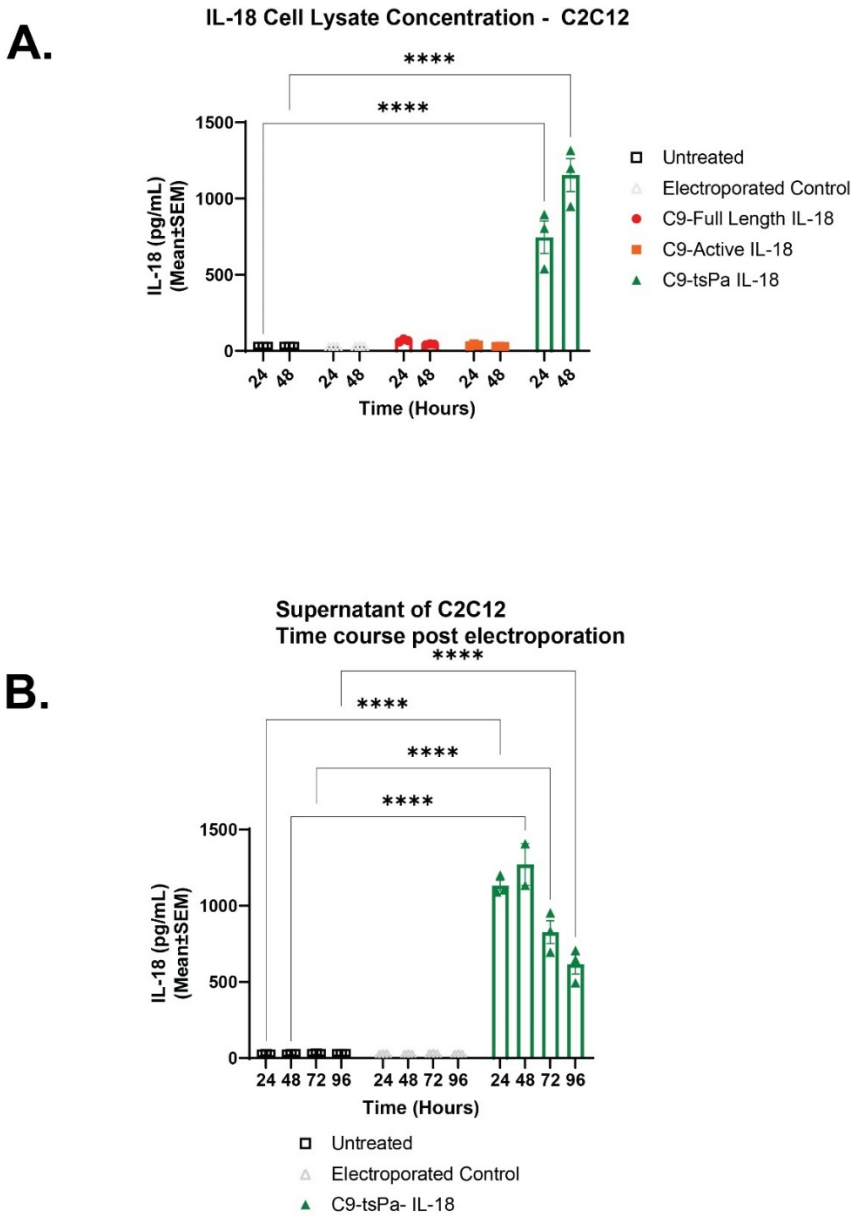

Figure 6. IL-18 RNA replicon validation in electroporated C2C12 supernatant and cell lysate by ELISA.

A. *IL-18 concentrations in the cell lysate of electroporated I µg of Full-Length IL-18, Active IL-18, and tsPa IL-18 RNA replicons.****P<0.0001 by ordinary two-way ANOVA using Dunnett's multiple comparison's tests, with a single pooled variance.* ***B.*** *Time course of IL-18 concentrations secreted in supernatant cell media post electroporation. ****P-value<0.0001 using ordinary two-way ANOVA with Dunnett's multiple comparisons test, with individual variances computed for each comparison.*

RAW264.7 cells produced an average of 111.9 pg/mL and 662.3 pg/mL of Full-Length IL-18 and tsPa IL-18 respectively at 24 hours, with the tsPa IL-18 construct producing more IL-18 as expected due to the enhanced secretory signal peptide compared to the native Full-Length IL-18 RNA replicon. RAW264.7 cells made little to no Active IL-18 that was detectable in the cell media supernatant compared to untreated control by ELISA (Figure 7A). Cell lysates of RAW264.7 macrophages showed IL-18 production within the cell for groups that received Full-Length IL-18 and tsPa IL-18 RNA replicons which averaged 523.7 pg/mL and 1,106.7 pg/mL respectively peaking at 24 hours and decreased by 48 hours almost to baseline levels compared to untreated control ($p<0.0001$) (Figure 7B).

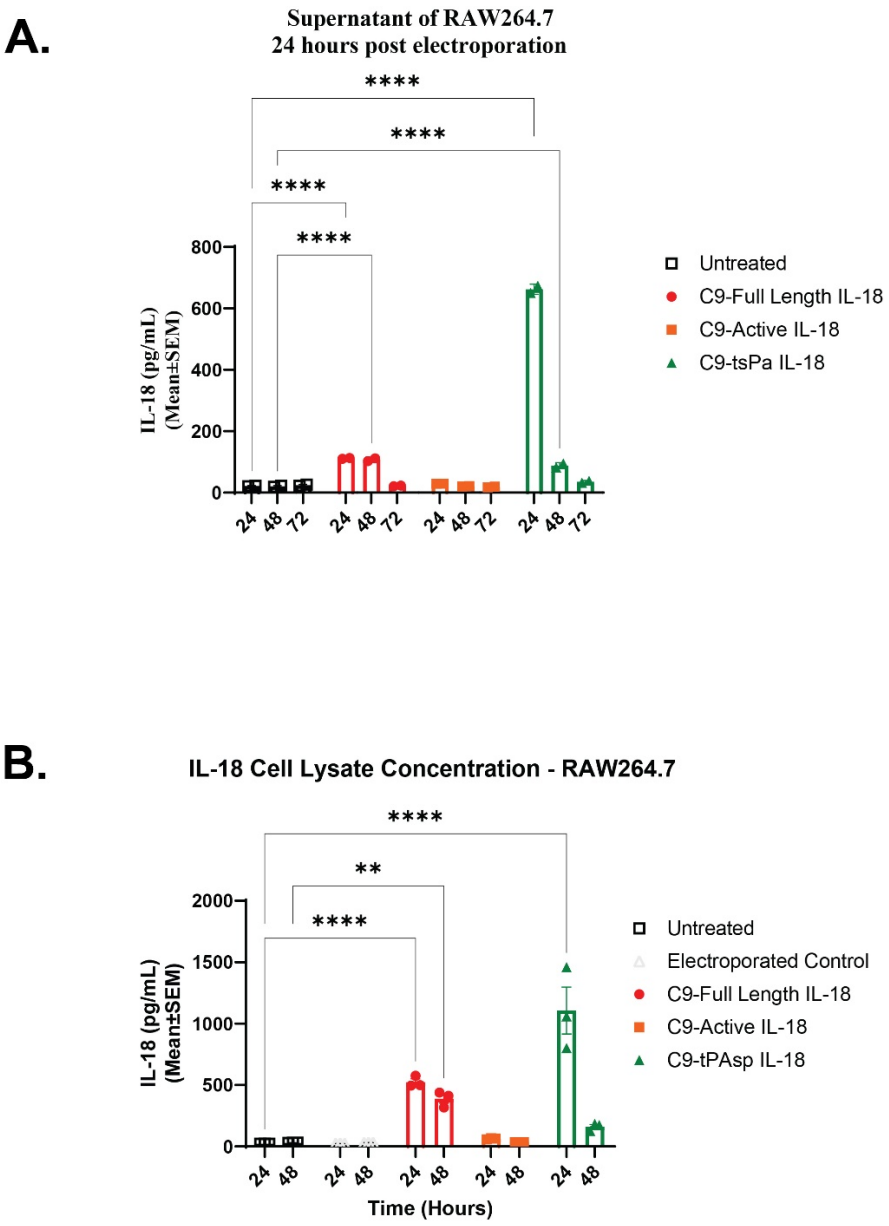

Figure 7. IL-18 RNA replicon validation in electroporated RAW264.7 supernatant and cell lysate by ELISA.

A. *Time course of IL-18 concentrations secreted in supernatant cell media post electroporation. .****P<0.0001 by ordinary two-way ANOVA using Dunnett's multiple comparison's tests, with individual variances computed for each comparison.* ***B.*** *IL-18 concentrations in the cell lysate of electroporated I µg of Full-Length IL-18, Active IL-18, and tsPa IL-18 RNA replicons.****P-value<0.0001 **P-value=0.0023 using ordinary two-way ANOVA with Šídák's multiple comparisons test with a single pooled variance and exact P-values indicated.*

Quantification of lipid nanoparticle delivery method using mCherry RNA replicons in B16F10 and HEK Blue IL-18 model cell lines

Another experiment was designed to examine an alternative method of delivery using lipid nanoparticles to encapsulate RNA replicons and deliver them into the cytosol. To validate the lipid nanoparticle delivery system, mCherry RNA replicons were fabricated, encapsulated, and delivered in triplicate in B16F10 and HEK Blue IL-18 model cell lines (Figure 8A). Successful transfection of B16F10s and HEK Blue IL-18 cell lines with 1 μg of mCherry reporter RNA replicons by transfecting for 4 hours followed by a 24-hour recovery validated the protocol. To quantify successful transfection efficiency with this delivery vehicle method, mean fluorescence intensity was determined by flow cytometry (Figure 8B). Transfection efficiency was calculated in two different ways. One was by the percent of mCherry positive cells assessed by flow cytometry that was live but also by back-calculating using absolute counting beads that were added at the end and gated on during analysis (Figure 8C, Table 3, 4, and 5). The average transfection efficiency of mCherry positive cells for B16F10 was 96.60% compared to 1.04% of B16F10 cells transfected with blank lipid nanoparticles. For HEK Blue IL-18, average transfection efficiency reached 76.63% compared to 1.38% of HEK Blue IL-18 cells that only received blank lipid nanoparticles. By counting beads, similar values were obtained for B16F10 and HEK Blue IL-18. Back calculated transfection efficiency of mCherry positive cells by counting beads resulted in 88.75% and 74.33% respectively followed by 1.66% and 2.59% in the blank lipid nanoparticle arm.

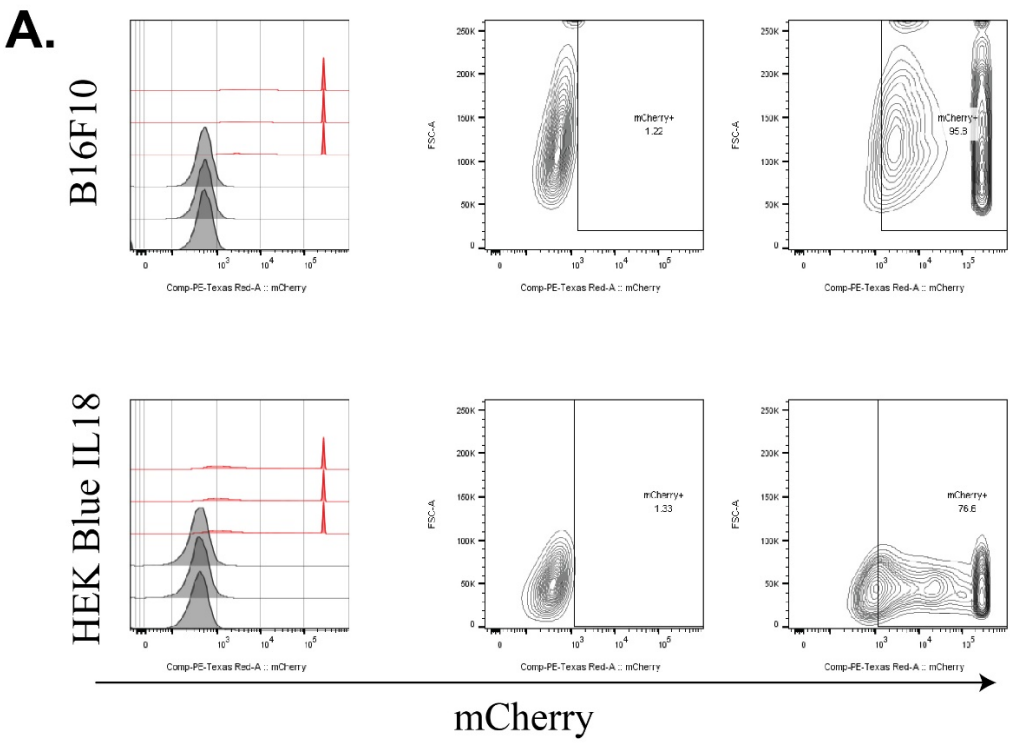

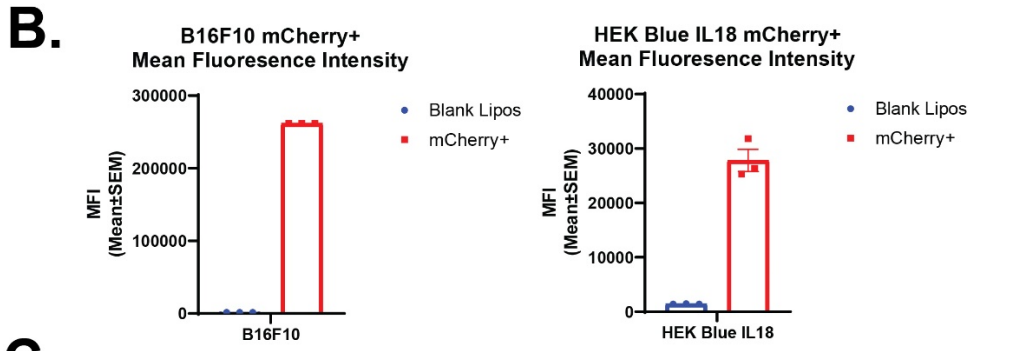

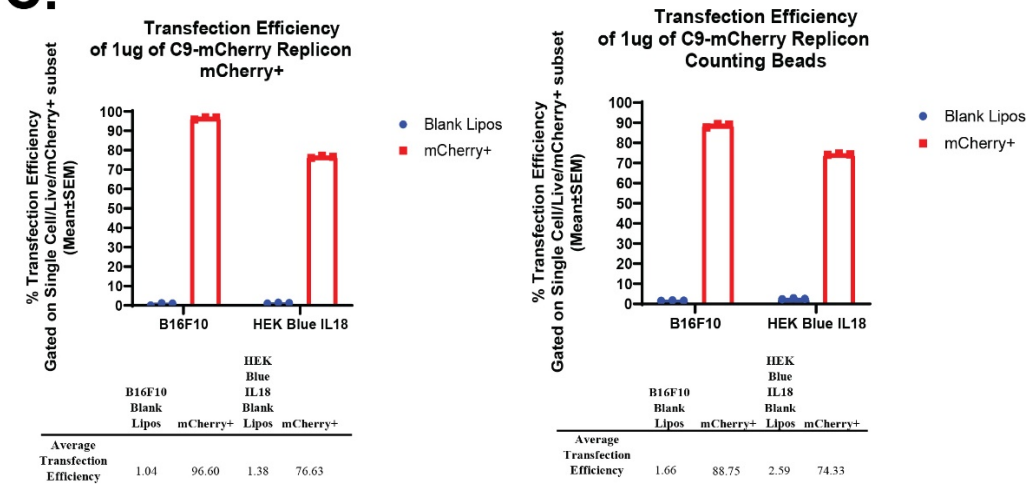

	B16F10 Blank Lipos	B16F10 mCherry+	HEK Blue IL18 Blank Lipos	HEK Blue IL18 mCherry+
Average Transfection Efficiency	1.04	96.60	1.38	76.63

	B16F10 Blank Lipos	B16F10 mCherry+	HEK Blue IL18 Blank Lipos	HEK Blue IL18 mCherry+
Average Transfection Efficiency	1.66	88.75	2.59	74.33

Figure 8. Validation of 1 μg of C9-mCherry replicons using lipid nanoparticle transfection.

A. *mCherry fluorescence signal expression by flow cytometry in B16F10 and HEK Blue IL18.* ***B.*** *Mean fluorescence intensity of mCherry.* ***C.*** *Quantification of transfection efficiency by mCherry fluorescence and absolute counting beads.*

B16F10	No mCherry (#Events)	mCherry+ (#Events)	Beads (#Events)	Abs. count no mCherry (cells/uL)	Abs. count of Live/mCherry+ (cells/uL)	Total (cells/uL)
Blank	16259.00	299.00	78798.00	106.26	1.95	108.22
Blank	15286.00	257.00	84107.00	93.60	1.57	95.17
Blank	19842.00	309.00	82432.00	123.96	1.93	125.89
mCherry+	937.00	6708.00	83297.00	5.79	41.47	47.27
mCherry+	821.00	6802.00	85901.00	4.92	40.78	45.70
mCherry+	699.00	5823.00	86248.00	4.17	34.77	38.94
HEK Blue IL18	**No mCherry (#Events)**	**mCherry+ (#Events)**	**Beads (#Events)**	**Abs. count no mCherry (cells/uL)**	**Abs. count of Live/mCherry+ (cells/uL)**	**Total (cells/uL)**
Blank	12855.00	316.00	84211.00	78.62	1.93	80.55
Blank	12511.00	366.00	81626.00	78.94	2.31	81.24
Blank	11945.00	309.00	80781.00	76.15	1.97	78.12
mCherry+	2690.00	7756.00	83832.00	16.53	47.65	64.17
mCherry+	2762.00	8162.00	81971.00	17.35	51.28	68.63
mCherry+	2846.00	8107.00	81543.00	17.97	51.20	69.18

B16F10	Total no mCherry+ (cells)	Total mCherry+ (cells)	Total (cells)	Percent Transfection Efficiency (%)
Blank	19127.51	351.75	19479.26	1.81
Blank	16847.73	283.26	17130.99	1.65
Blank	22313.58	347.49	22661.07	1.53
mCherry+	1042.77	7465.23	8508.01	87.74
mCherry+	885.98	7340.37	8226.35	89.23
mCherry+	751.29	6258.60	7009.89	89.28
HEK Blue IL18	**Total no mCherry+ (cells)**	**Total mCherry+ (cells)**	**Total (cells)**	**Percent Transfection Efficiency (%)**

Blank	14150.87	347.85	14498.72	2.40
Blank	14208.34	415.65	14623.99	2.84
Blank	13707.45	354.59	14062.04	2.52
mCherry+	2974.56	8576.45	11551.01	74.25
mCherry+	3123.51	9230.31	12353.82	74.72
mCherry+	3235.40	9216.23	12451.63	74.02

$$Absolute\ cell\ count\ \left(\frac{cells}{\mu L}\right) = \frac{Cell\ Count}{Beads\ (Events)} * Bead\ Concentration\ \left(\frac{Beads}{\mu L}\right)$$

Table 3. Percent transfection efficiency calculated by counting beads

This is the percent transfection efficiency calculated using counting beads with the following equation.

B16F10	**Cells/Single Cells/Live/mCherry+ | Freq. of Parent**
Blank	1.22
Blank	1.02
Blank	0.89
mCherry+	95.8
mCherry+	96.9
mCherry+	97.1
HEK Blue IL18	**Cells/Single Cells/Live/mCherry+ | Freq. of Parent**
Blank	1.33
Blank	1.43
Blank	1.39
mCherry+	76.6
mCherry+	77.2
mCherry+	76.1

Table 4. Percent transfection efficiency calculated by gating on mCherry+ subset

The table contains the mCherry+percent frequency of B16F10 and HEK Blue IL18 compared to blank control.

Sample	Hydrodynamic diameter [nm]
Blank Lipofectamine	765.9 ± 71.1
mCherry	648.8 ± 25.1
Full Length IL18	720.0 ± 19.7
Active IL18	712.7 ± 18.0
tsPa IL18	735.5 ± 14.6
scIL12 and Full Length IL18	850.6 ± 31.9
scIL12 and Active IL18	663.7 ± 33.6
scIL12 and tsPa IL18	815.4 ± 34.0
scIL12 MSA	759.5 ± 55.7

Table 5. Comparison of lipofectamine encapsulated replicons

Hydrodynamic measurement on DLS of lipid nanoparticles formulated with RNA replicons.

Validation of IL-18 RNA replicons in HEK Blue IL-18 reporter cell line for bioactivity by QUANTI Blue SEAP detection assay

Given the high transfection efficiency with mCherry and Lipofectamine MessengerMAX, it was hypothesized that lipid nanoparticles could efficiently encapsulate and deliver IL-18 RNA replicons. To validate the bioactivity of IL-18 produced by IL-18 RNA replicons, HEK Blue IL-18 were transfected with IL-18 RNA replicons using lipid nanoparticles and quantified using a QUANTI Blue colorimetric assay detecting for SEAP alkaline phosphatase production in the supernatant. After a 4-hour transfection followed

by 24 and 48-hour recovery, SEAP secretion that was statistically significant compared to untreated controls was detected in the tsPa IL-18, scIL-12 and Active IL-18, and scIl-12 and tsPa IL-18 ($p<0.0001$) groups suggesting IL-18 was being produced after transfection (Figure 9). This result is representative of two independent experiments with each condition run in triplicate.

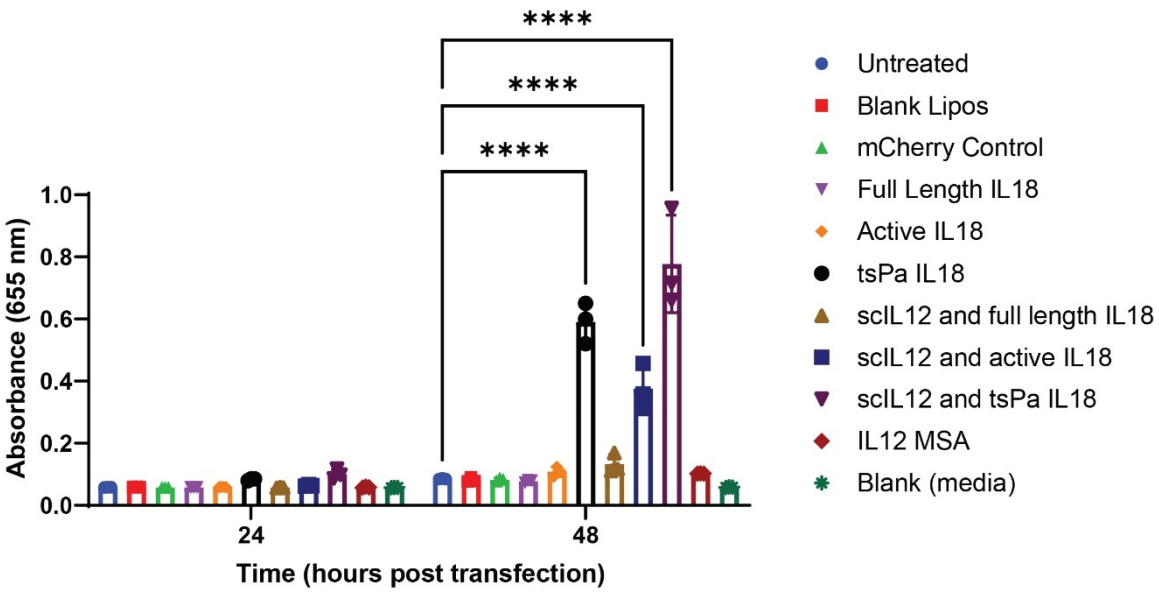

Figure 9. Functional SEAP reporter assay using engineered HEK Blue IL-18 cell line.

*Colorimetric analysis of SEAP production 24 and 48 hours post-transfection of 1ug of RNA replicon to HEK Blue IL18 via Lipofectamine MessengerMAX. The supernatant was incubated for 1 hour at 37℃ in QUANTI Blue before absorbance was measured at 655 nm. ****P-value<0.0001 by ordinary two-way ANOVA with Dunnett's multiple comparisons test, with a single pooled variance.*

This dataset provides evidence to support that IL-18 RNA replicons can be delivered *in vitro* through electroporation or lipid nanoparticle delivery into a target cell. Furthermore, these experiments definitively support that tsPa IL-18 replicons can be detected and secreted in the cell supernatant which was also seen in a dual construct format

of scIL-12 and tsPa IL-18. Full-Length IL-18 and dual construct scIL-12 and Full-Length IL-18 did not secrete as expected. Active IL-18 did not secrete as expected in this assay but dual construct scIL-12 and Active IL-18 demonstrated that IL-18 can be bioactive without a signal peptide (Figure 9).

Discussion

The experiments conducted in this chapter focused on supporting the claim that IL-18 can be produced in a bioactive form from replicons transfected into cell lines, without the requirement for a signal peptide. Before we could address this question, validation studies were conducted to ensure the replicons were constructed properly and to verify a transfection system for downstream applications. To do so, C2C12 and RAW264.7 were chosen to pilot test and validate the synthesized IL-18 RNA replicons. C2C12 is a common immortalized murine myoblast model used to model drug administration into muscle tissue like RNA vaccines administered intramuscularly (Park et al., 2021). RAW264.7 macrophages are also commonly used to test the delivery of lipid nanoparticles. For example, strategies have been developed to genetically reprogram macrophages to elicit anti-tumor functions using mRNA (F. Zhang et al., 2019).

Cell lysates were chosen to examine the production and determine whether Active IL-18 could be detected by ELISA. Results showed no detection of IL-18 from the Full-Length IL-18 or the Active IL-18 RNA replicon in C2C12 cells when delivered by electroporation in the cell media supernatant or cell lysate (Figure 6). We do see some IL-18 in the cell lysate of RAW264.7 transfected with Full-Length IL-18 RNA replicon (Figure 7B). Consistently, we see tsPa IL-18 being expressed in C2C12 and RAW264.7 cell lines as expected in both the cell media supernatant and cell lysate (Figure 6 and Figure

7). Some limitations of this method may lie with how the electroporation was done since the RNA replicons were diluted in a resuspension buffer and delivered directly. Because the RNA replicons were not encapsulated to protect from potential RNase degradation during the electroporation, the procedure may have led to insufficient delivery into the cells of interest. Electroporation has been described to decrease cell viability which limits protein production and translation (Donahue et al., 2019). These data motivated the next few studies for a more translational approach.

Optimization of lipid nanoparticle encapsulation studies was conducted to test if better transfection efficiency could be achieved in cell lines previously tested with LNP transfection (Li et al., 2019, 2020). B16F10 melanoma was chosen as the model cell line for lipid nanoparticle encapsulation delivery studies. To gauge transfection efficiency and optimize a protocol for lipofectamine, pilot studies were run testing 0.75 μL of Lipofectamine per well and 1.5 μL of Lipofectamine per well based on the recommendation from the manufacturer's protocol. The lower dose was chosen to help mitigate toxicity concerns from long incubation times and because the levels of IL-18 produced were not different (data not shown). Transfection studies using mCherry RNA replicons helped gauge the selected protocol's efficiency in delivering encapsulated RNA replicons into B16F10. HEK Blue IL18—a reporter IL-18 cell line—showed slightly lower transfection efficiency (Figure 8).

Limitations of this experiment include the potential loss of cells during the harvest because B16F10s are an adherent line. Trypsin was not used to detach cells from the well. This was taken into consideration for future extracellular staining of receptors on the surface and preserve structural integrity. Mechanical removal of B16F10 from the well

leads to poorer recovery and cell loss. Moreover, when using Lipofectamine MessengerMAX to encapsulate RNA replicons, the hydrodynamic diameter was between 600-800 nm (Table 4) but was similar to a published report that encapsulated plasmids for delivery into stem cells using Lipofectamine 2000 (Wallenstein et al., 2010). This is important to consider when determining transfection efficiency as the cellular uptake of nanomaterials depends on the method of delivery, size, shape, charge, surface modifications, and colloidal stability (Donahue et al., 2019, 2020).

To test bioactivity and whether the requirement of proteolytic cleavage of the propeptide precursor was necessary to elicit activity, three different RNA replicons were designed. Full-Length IL-18 would require the cleavage of the propeptide precursor sequence whereas Active IL-18 and tsPa IL-18 would not. Active IL-18 does not have a propeptide sequence and tsPa IL-18 is more efficient at secreting protein due to the tissue plasminogen sequence that replaced the propeptide sequence. In the dual constructs, scIL-12 and Active IL-18 were being detected as SEAP was being secreted by HEK Blue IL-18 cells in the culture but not in the Active IL-18 alone scenario (Figure 9). Moreover, compared to the scIL-12 and tsPa IL-18 group, the amount of SEAP detected was lower. It is hypothesized that although Active IL-18 is bioactive, it relies heavily on the gene upstream for secretion because it does not have a signal peptide or enhanced secretory signal peptide. This is further exemplified in Chapter IV when looking at the synergy between IL-12 and IL-18 in the context of immunogenic cell death and pyroptosis.

Chapter IV.

Synergistic effects of scIL-12 and IL-18 RNA replicons

Introduction

Immunomodulation has the potential to generate robust anti-tumor activity but induction of immunological responses requires signaling that may be absent in the tumor microenvironment. Numerous immunomodulators such as IL-2, α-CTLA-4, and α-PD1/α-PDL1 therapy have seen some success in the clinic for indications varying from melanoma to kidney cancer as a monotherapy (Larkin et al., 2015; Tang & Harding, 2019). However, these therapies fall short due to a highly suppressive tumor microenvironment that is constantly changing over time (Bedard et al., 2013). A small subset of patients does respond to improve five-year survival rates, a metric commonly used to gauge treatment effectiveness. To combat more aggressive forms of cancer, it is important to consider alternatives such as combination therapy (Larkin et al., 2019). RNA therapy offers a platform that is bolstered by the potential that they can be tunable—like an on-off switch—which would give clinicians the flexibility to control dose to mitigate potential side effects due to treatment from a bolus administration or multiple-dose regimens (Chung et al., 2015).

Our group previously demonstrated RNA replicons encoding for scIL-12 MSA and scIL-12 lumican encapsulated in a lipid nanoparticle and delivered intratumorally were able to induce potent *in vivo* responses due to ICD in B16F10 melanoma. Similar responses

were reported *in vitro* (Li et al., 2020). Here we expand upon the use of ICD as a method to test for bioactivity of IL-18 replicons *in vitro* in this proof-of-concept co-culture system using transfected B16F10 melanoma cells and naïve splenocytes. We found increased production of IFN-γ upon delivery of IL-12 and IL-18 dual cytokine payload replicons in a subset of NK cells bearing higher levels of IL-18 receptor expression, compared to single replicon alone by flow cytometry. IFN-γ secreted in the supernatant was quantified by ELISA from the same samples to support the proof-of-concept. To supplement this finding, splenocytes were stimulated with exogenous cytokines to mimic what was seen in the co-culture system and look for IL-18 receptor expression upon IL-12 or IL-2 stimulation as well as IFN-γ production (Nakanishi, 2018; Yoshimoto et al., 1998). Interestingly, ICD and pyroptosis may have played a role in the induction of IFN-γ based on the previous findings (Li et al., 2020).

Results

Flow cytometry analysis of lipid nanoparticle delivered IL-18 RNA replicons show the production of IL-18 and IL-12 in a B16F10 melanoma model

B16F10 cells were transfected with IL-18 RNA replicons following the protocol described in Chapter II Materials and Methods. Flow cytometry analysis of transfected cells stained with FITC labeled IL-18 and PE-labeled IL12p40 gated on Single Cells and Live-cell subset by a live dead exclusion dye showed a shift from the single positive gates into the double-positive quadrant compared to untreated and blank lipid nanoparticle controls in groups receiving the dual RNA replicon constructs. Specifically, groups that

received scIL-12 and Full-Length IL-18, scIL-12 and Active IL-18, and scIL-12 and tsPa IL-18 showed staining for both IL-18 and IL-12p40 (Figure 10A).

For single IL-18 RNA replicon arms, the frequency of IL-18 positive B16F10 cells gated on live cells was an average of 20% in the Full-Length Il-18 group whereas Active IL-18 and tsPa IL-18 groups showed an average frequency of cells positive for IL-18 of around 10% (Figure 10B). tsPa IL-18 transfected live B16F10 cells showed a lower overall frequency of IL-18, the group had the highest average mean fluorescence intensity whereas Full-Length IL-18 and Active Il-18 were significantly lower by about 2/3 but still statistically significant ($p<0.0001$) when compared to untreated control (Figure 10B). The frequency of IL-12p40 of live B16F10 cells was highest in the IL-12 MSA RNA replicon cohort with an average mean of around 30% compared to the dual constructs scIL-12 and Full-Length IL-18, scIL-12 and Active IL-18, and scIL-12 and tsPa IL-18 with an average mean of around 20%. IL-12 MSA had the highest mean fluorescence intensity of IL-12p40 compared to the other groups. The frequency of live cells producing IL-18 and IL-12 was an average of 7-8% for all dual construct arms.

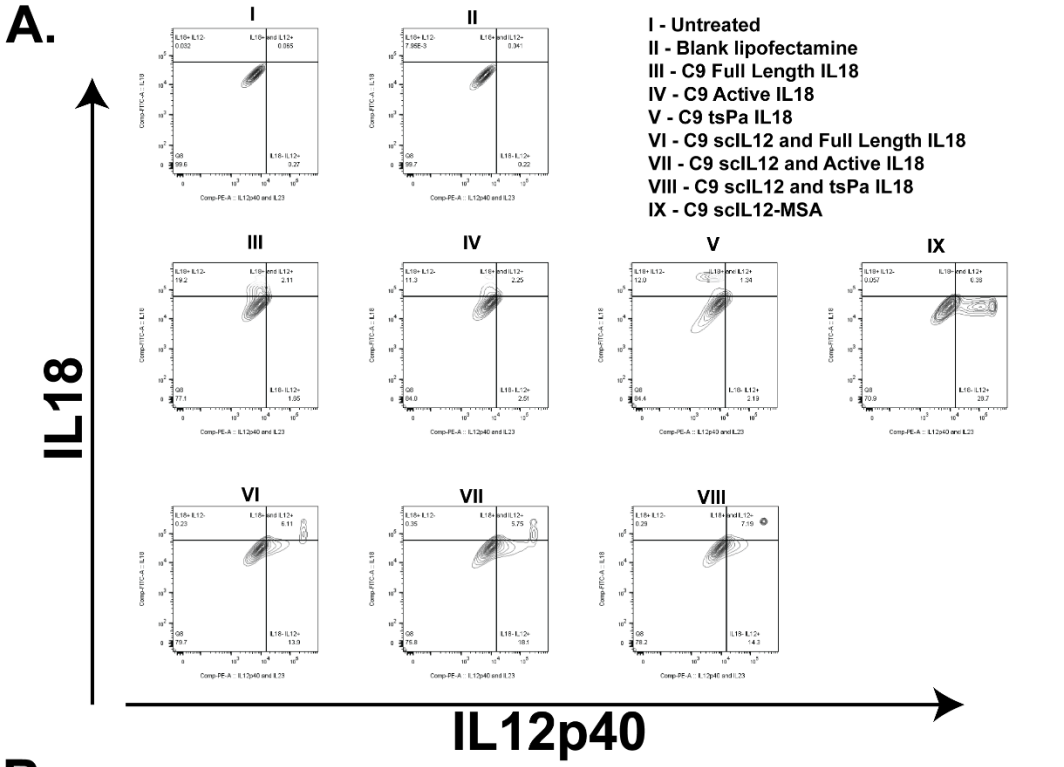
A.
I
II
III
IV
V
IX
VI
VII
VIII
I - Untreated
II - Blank lipofectamine
III - C9 Full Length IL18
IV - C9 Active IL18
V - C9 tsPa IL18
VI - C9 scIL12 and Full Length IL18
VII - C9 scIL12 and Active IL18
VIII - C9 scIL12 and tsPa IL18
IX - C9 scIL12-MSA
IL18
IL12p40

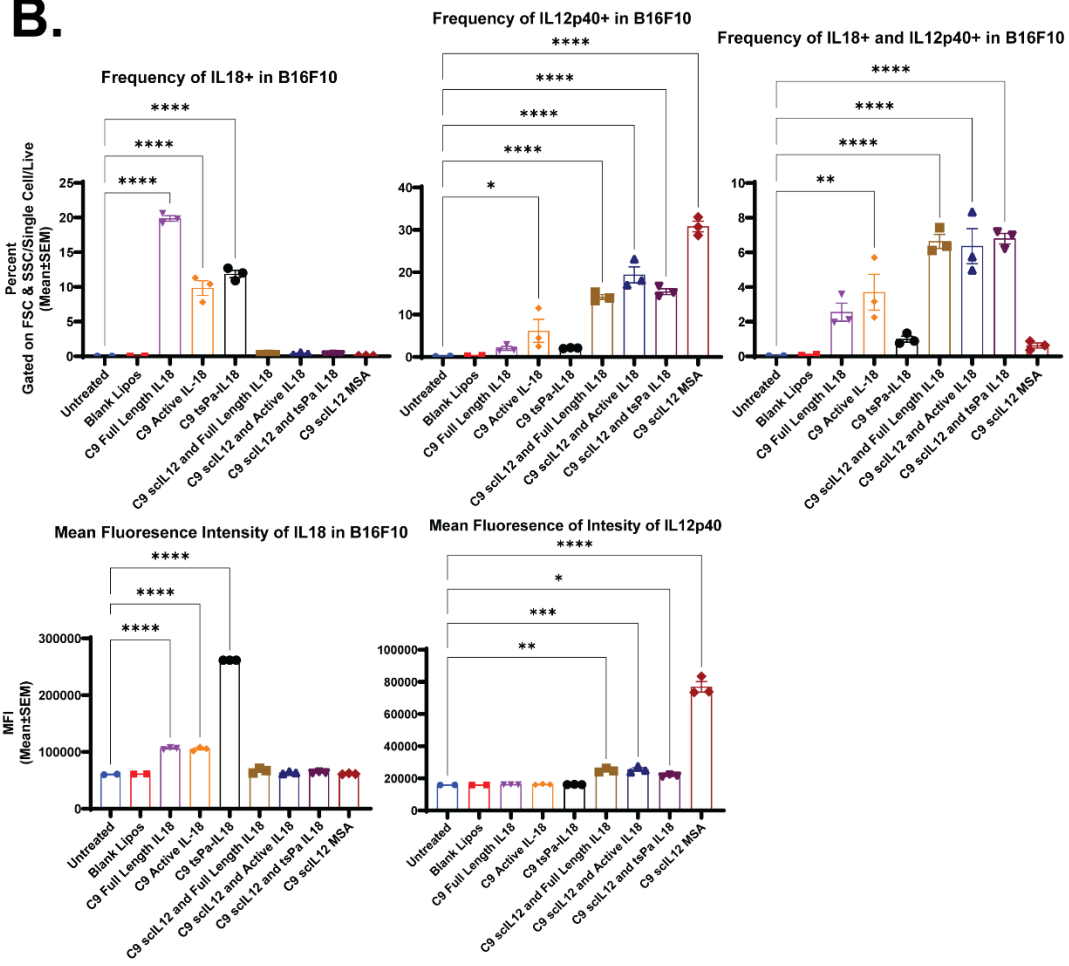
B.
Frequency of IL18+ in B16F10
Frequency of IL12p40+ in B16F10
Frequency of IL18+ and IL12p40+ in B16F10
Percent Gated on FSC & SSC/Single Cell/Live (Mean±SEM)
Mean Fluoresence Intensity of IL18 in B16F10
Mean Fluoresence of Intesity of IL12p40
MFI (Mean±SEM)
Untreated
Blank Lipos
C9 Full Length IL18
C9 Active IL-18
C9 tsPa-IL18
C9 scIL12 and Full Length IL18
C9 scIL12 and Active IL18
C9 scIL12 and tsPa IL18
C9 scIL12 MSA

Figure 10. Flow cytometry analysis of IL-18 and IL-12 expression in B16F10 post-24-hour lipofectamine transfection.

A. *Example contour plots (n=3 per construct) of IL-18, IL-12, and IL-18/IL-12 positive subsets gated on FSC vs SSC/Single Cell/Live.* ***B.*** *Frequency and mean fluorescence intensity of IL-18, IL-12, and IL-18/IL-12 in B16F10 gated on FSC vs SSC/Single Cell/Live. Statistics were calculated using ordinary one-way ANOVA with Dunnett's multiple comparisons test, with single pooled variance and exact P values are indicated. Frequency IL-18 and IL-12 Statistics: ****P-value<0.0001 **P-value=0.0045 Frequency IL-18 Statistics: ****P-value<0.0001 Frequency of IL-12p40: ****P-value<0.0001 *P-value=0.0457 MFI IL-12 Statistics: ****P-value<0.0001 ***P-value=0.0008 **P-value=0.0013 *P-value=0.0498 MFI IL-18 Statistics: ****P-value<0.0001*

The frequency of IL-18 positive events was reported showing a significant increase compared to untreated control from the Full-Length IL-18, Active IL-18, and tsPa IL-18 constructs ($p<0.0001$ for all three single RNA replicon constructs) (Figure 10B). Similar results were seen from the dual constructs where IL-12p40 was detected and the frequency of IL-12p40 was statistically significant compared to untreated control ($p<0.0001$ for all dual constructs). (Figure 10B). RNA replicons encoding scIL-12 MSA alone showed the greatest frequency of events when looking at the IL12p40 quadrant. When looking at the double-positive gate, we see a small fraction of cells that stained positive for both IL-18 and IL-12 with the frequency being highest in the dual constructs compared to untreated control. By MFI, we see a shift in the single IL-18 RNA replicons that were statistically significant for IL-18 ($p<0.0001$ for all single RNA replicon constructs). There was a modest increase of IL-12p40 in the dual replicons compared to control whereas the scIL-12 MSA showed a great increase in MFI.

Lipid nanoparticle encapsulated RNA replicons transfected B16F10 and cocultured *in vitro* with naïve total murine splenocytes show IFN-γ production in response to IL-12 and IL-18

Motivated by results from the previous experiment, B16F10 cells were seeded and transfected with IL-18 RNA replicons, followed by co-culture with Cell Trace Violet labeled naïve splenocytes harvested from C57BL/6 female mice for 24 hours. Gating strategy began with FSC vs SSC gated on lymphocytes, Single Cell gate, murine CD45+ Cell Trace labeled+ lymphocytes to differentiate between unlabeled B16F10 melanoma cells, CD4 vs CD8, CD3 by CD11b, followed by NK1.1 by CD11b and subdivided between CD3- CD11b+ for myeloid cells and CD3- CD11b+ NK1.1 for NK cells, lastly gating on CD3- NK1.1+ IL18R+ looking at IFN-γ production (Figure 11). This staining panel did not have a B-cell specific marker or live dead Aqua for the exclusion of dead cells due to Cell Trace Violent labeled splenocytes causing spectral overlap.

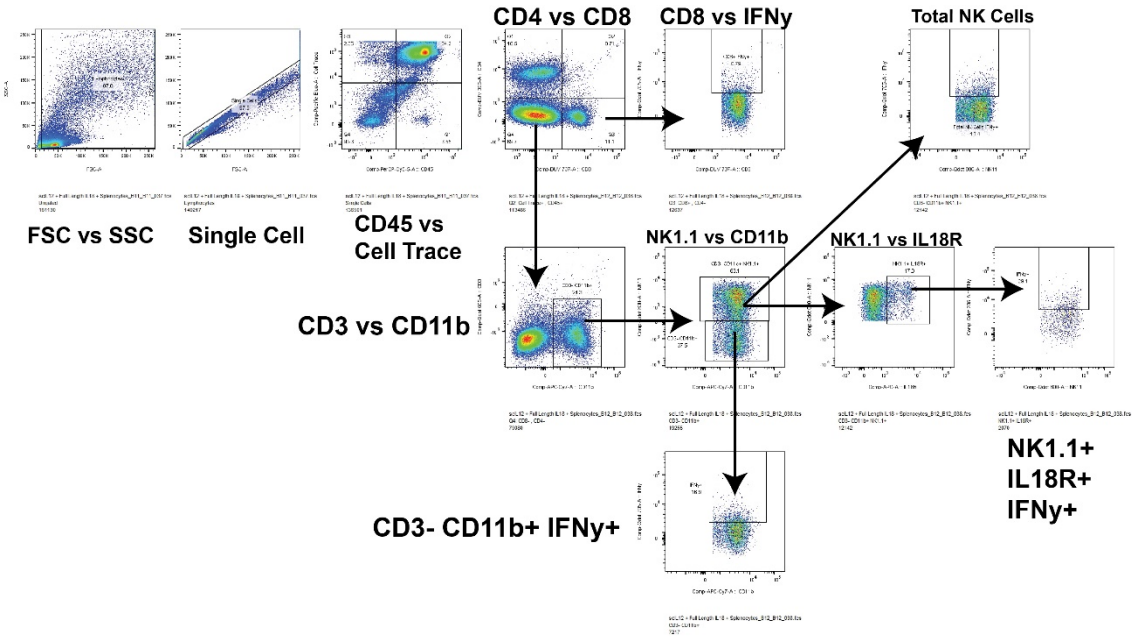

Figure 11. Example gating strategy used for NK1.1+ IL18R+ subset for B16F10 cocultured with splenocytes.

Flow cytometry gating strategy used for identification of CD3- CD11b myeloid cells, CD3- CD11b+ NK1.1+ NK cells, and the NK1.1+ IL18R+ subset.

Flow cytometry analysis of cells from this co-culture revealed an IFN-γ production shift in a subset of NK1.1+ IL18R+ cells compared to untreated control and absent in single cytokine-producing IL-18 RNA replicons (Figure 12A). As expected, IL-12 MSA induced IFN-γ responses within the coculture (Figure 12A). Similar IFN-γ shifts were seen in CD8+ T-cells, CD3- CD11b+ myeloid cells, and CD3- NK1.1+ total NK cells (Figure 12B). Cell media supernatant was saved 6 hours post-transfection and 24 hours post-transfection to quantify IFN-γ production by ELISA. Little to no IFN-γ was detected by ELISA at 6 hours (data not shown). The IFN-γ ELISA data corroborates the findings observed by flow cytometry at 24 hours where increases in IFN-γ production were primarily noted in the

dual constructs with scIL-12 and Full-Length IL-18 that averaged 2,232.8 pg/mL followed by scIL-12 and tsPa IL-18 averaging 762.2 pg/mL and lastly scIL-12 and Active IL-18 averaging 336.0 pg/mL (Figure 13).

A.

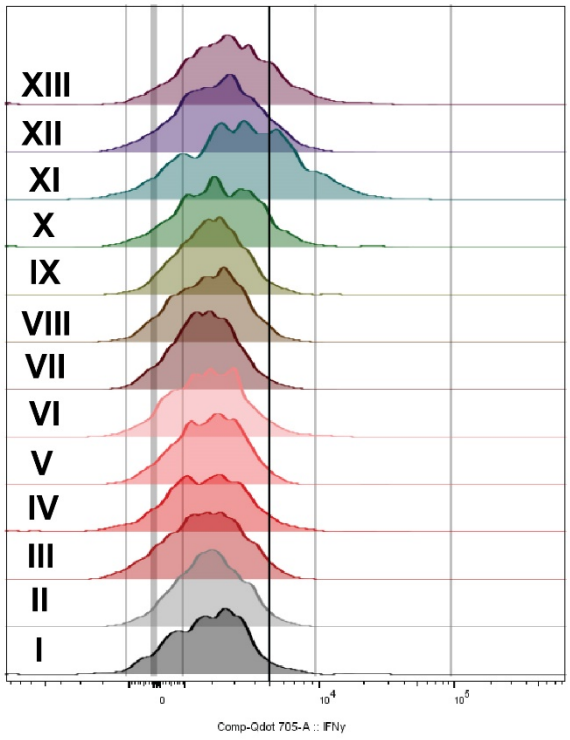

	Sample Name	Subset Name	Count
	scIL12 +tsPa IL18 + Splenocytes_C2_C02_040.fcs	NK1.1+ IL18R+	1744
	scIL12 + Active IL18 + Splenocytes_B8_B08_034.fcs	NK1.1+ IL18R+	1546
	scIL12 + Full Length IL18 + Splenocytes_B12_B12_038.fcs	NK1.1+ IL18R+	2070
	scIL12 MSA_C5_C05_043.fcs	NK1.1+ IL18R+	1416
	tsPa IL18 + Splenocytes_B4_B04_030.fcs	NK1.1+ IL18R+	1146
	Active IL18 + Splenocytes_B2_B02_028.fcs	NK1.1+ IL18R+	1308
	Full Length IL18 + Splenocytes_A10_A10_024.fcs	NK1.1+ IL18R+	1604
	BFA Only_G1_G01_047.fcs	NK1.1+ IL18R+	1352
	PMA Iono Only_F1_F01_045.fcs	NK1.1+ IL18R+	934
	PMA Iono + BFA_H1_H01_049.fcs	NK1.1+ IL18R+	818
	mCherry + Splenocytes_A7_A07_021.fcs	NK1.1+ IL18R+	1388
	Blank + Splenocytes_A4_A04_018.fcs	NK1.1+ IL18R+	1440
	Untreated + Splenocytes_A1_A01_015.fcs	NK1.1+ IL18R+	823

XIII scIL-12 and tsPa IL-18
XII scIL-12 and Active IL-18
XI scIL-12 and Full Length IL-18
X scIL-12 MSA
IX tsPa IL-18
VIII Active IL-18
VII Full Length IL-18
VI BFA Only
V PMA/Iono Only
IV PMA/Iono+BFA Control
III mCherry Control
II Blank Lipos
I Untreated

B.

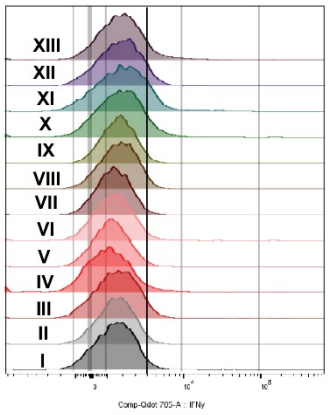

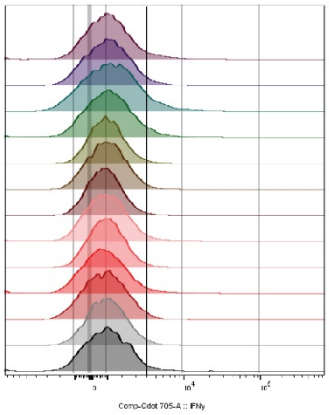

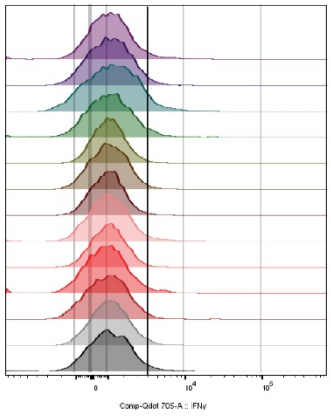

CD8+ T-cells

CD3- NK1.1+ Total NK Cells

CD3- CD11b+ Myeloid Cells

Figure 12. Histograms of IFN-γ production in different immune subsets of B16F10 coculture of representative samples.

A. IFN-γ production of NK1.1+ IL18R subset (n=3 technical triplicates). Dark line depicts where a positive gate was drawn. B. IFN-γ production in CD8+ T-cells, CD3- CD11b+ NK1.1+ Total NK cells, and CD3- CD11b+ myeloid cell subsets. (n=3 technical triplicates). The dark line depicts where the positive gate was drawn.

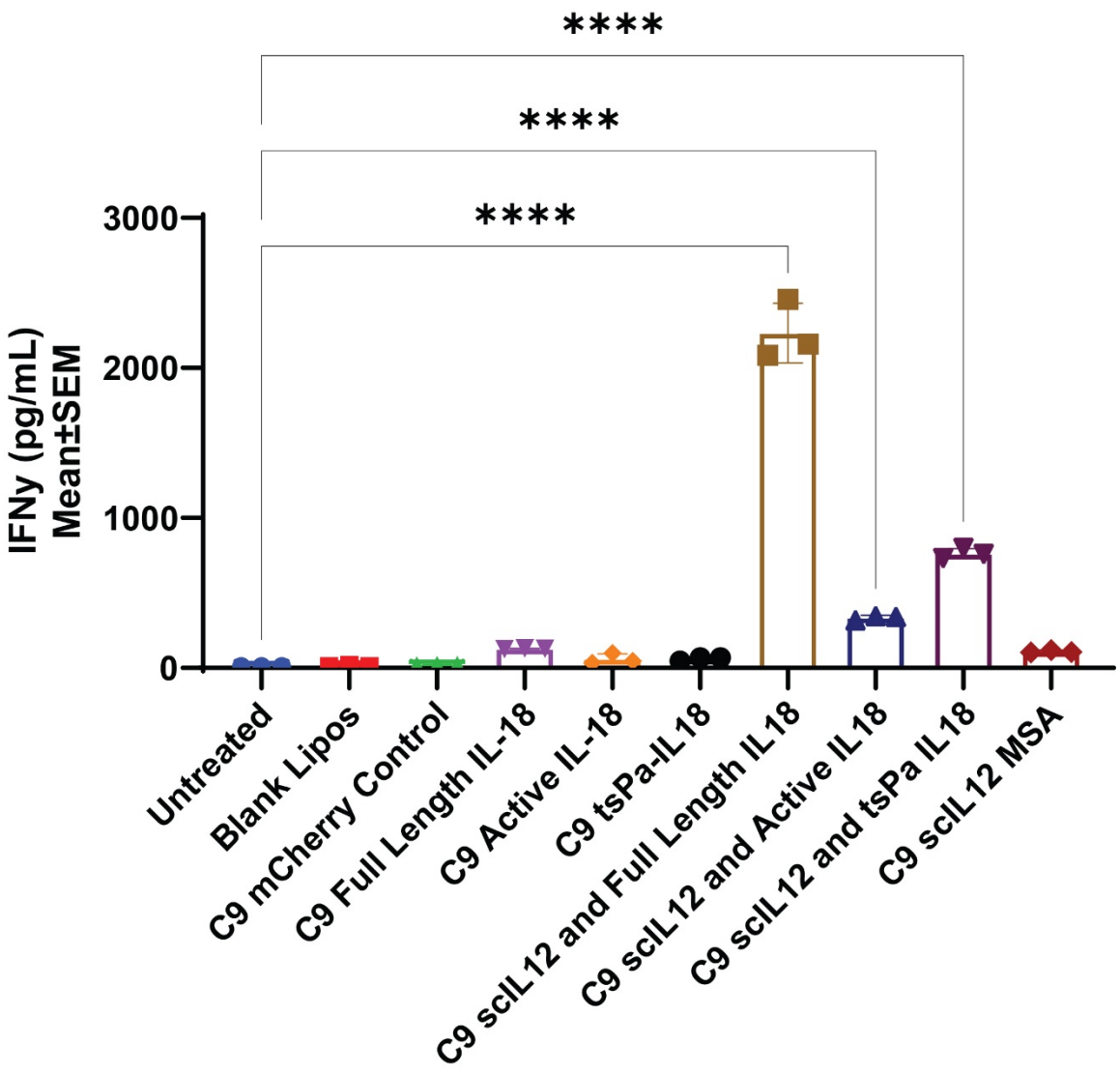

Figure 13. Increased IFN-γ production in IL-12 and IL-18 dual constructs in B16F10 coculture with fresh naïve splenocytes after 24 hours by ELISA.

*Quantification of IFN-γ production secreted in the supernatant by ELISA. ****P-value<0.0001 using ordinary one-way ANOVA with Dunnett's multiple comparisons test, with single pooled variance.*

Cytokine stimulation assay validation of synergism of IL-12 and IL-18

Concurrently in a separate study, a cytokine stimulation assay experiment was designed to mimic what was seen in the co-culture experiment and validate IL-12 and IL-18 synergism triggering the production of IFN-γ by flow cytometry. Cells were gated on Single Cell/Live/CD45+/CD3- CD11b+/NK1.1+/IL18R+/IFN-γ. The NK1.1+ IL-18R+ subset showed that stimulation with either IL-2 or IL-12 led to the upregulation of IL18R compared to untreated control but not IFN-γ (Figure 14.).

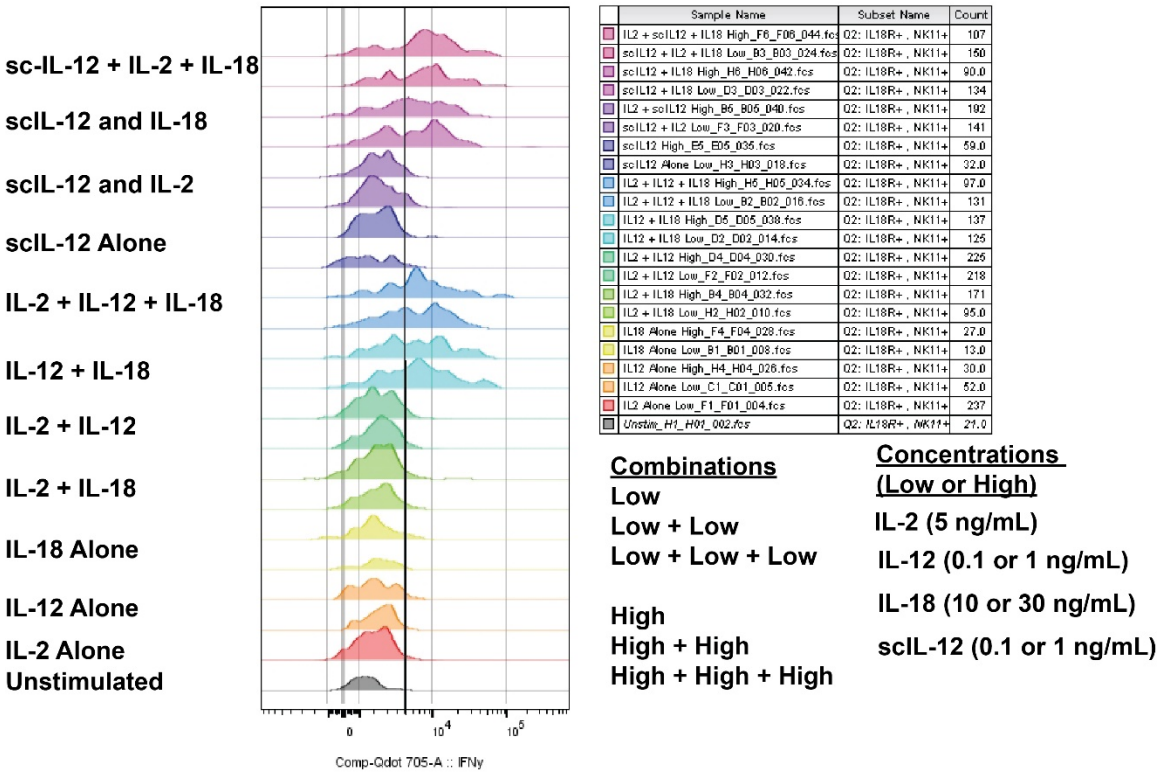

Figure 14. *In vitro* cytokine stimulation assay with recombinant IL-2, IL-12, IL-18, and scIL-12 at different doses for 24 hours

Representative schematic of cytokine stimulation assay of 100,000 splenocytes (n=2 technical replicates per condition) for 24 hours in vitro. Recombinant IL-2 final concentration was 5 ng/mL, recombinant IL-12/scIL-12 final concentration was either 0.1 ng/mL (low) or 1 ng/mL (high), and recombinant IL-18 final concentration was 10 ng/mL (low) or 30 ng/mL (high). Black line represents positive gate cut-off.

CD8+ T-cells were also not producing IFN-γ upon single administration of any cytokine regardless of dose level (data not shown). When IL-12 was combined with IL-2, IL-18R was upregulated more profoundly with a slight increase in the frequency of IFN-γ in both the NK1.1+ IL18R+ and CD8+ compartment. When IL-12 and IL-18 were spiked together, a strong robust IFN-γ response was produced in response to the stimuli (Figure

14)). This was also noted when IL-2, IL-12, and IL-18 were added together in combination (Figure 14). scIL-12 showed similar results when given at the same dose as recombinant IL-12 (Figure 14). Only when all 3 cytokines were combined, there was IFN-γ expression induced in CD8+ T-cells (data not shown). These findings together with the previous studies presented in this chapter support the hypothesis of IL-12 and IL-18 synergy.

Discussion

IL-12 and IL-18 synergy is well established in the literature and still plays an important role in our understanding of key drivers of robust immunological responses in the context of cancer (Nakahira et al., 2002; Nakanishi, 2018; Tominaga et al., 2000). As presented in the earlier section of this chapter, in our experiments IL-18 alone was not able to induce IFN-γ expression in splenocytes in an *in vitro* co-culture setting which corresponds with published literature (Nakanishi, 2018, Figure 12). Interestingly, not all IL-12 encoding RNA replicons were able to induce IFN-γ which was not expected because it is well understood that IL-12 induces IFN-γ production in CD8+ T-cells, natural killer cells, and macrophages (Leonard et al., 1997; Vignali & Kuchroo, 2012, p. 12). Dual construct scIL-12 and Active IL-18 and IL-12 MSA induced the least amount of IFN-γ compared to that of scIL-12 and Full-Length IL-18 and scIL-12 and tsPa IL-18 (Figure 12 and Figure 13). In the latter cases that induced robust IFN-γ, IL-18 acted as a costimulatory cytokine synergizing with IL-12 (Kohno et al., 1997; Nakahira et al., 2002; Tominaga et al., 2000, Figure 12). One possible hypothesis for the low production of IFN-γ—or lack thereof—could be due to anergy.

Traditionally, activation of T-cells requires two signals: one from a specific antigen and another by a costimulatory signal (Bretscher, 1999). Cytokines act as an inflammatory

signal 3 to extend the duration of the response (Curtsinger et al., 1999). It has been shown that out of sequence signaling by a strong systemic cytokine response can lead to anergy and paralysis of CD4+ T-cells unable to respond to antigen leading to defective proliferation and activation (Sckisel et al., 2015). In the B16F10 co-culture system, splenocytes were added 24 hours post-transfection of B16F10 with RNA replicons. In the dual construct conditions, IL-12 is secreted in high quantities in the cell media supernatant by IL-12p70 ELISA (data not shown) and has also been previously described (Li et al., 2020). This would mean naïve splenocytes were added immediately into an environment containing highly concentrated cytokine and incubated for an additional 24 hours before quantification of IFN-γ and flow cytometry analysis. In the situations where IL-18 was present, IL-18 acted as a costimulatory signal to overcome the initial burst of cytokine present and could explain why IFN-γ was detected by ELISA in the scIL-12 and Active IL-18 case but not the IL-12 MSA (Figure 13). Thus, developing a way to control the amount of cytokine produced is essential to prevent overstimulation or unwanted side effects allowing for better control and tunable kinetics (Andries et al., 2015; Chung et al., 2015; Slusarczyk et al., 2012; Wagner et al., 2018).

Another possible explanation is that in the context of a viral infection, IFN-γ differs based on the cytokine combination present. It also differs based on the type of viral infection. Despite non-viral RNA replicons do not produce infectious progeny, they are—however—derived from viral sequences making them "virus-like". In the literature, a study was conducted examining two subsets of CD8+ T-cells, CD8 effectors, and CD8 memory, showing that the cytokine milieu in which the cells are in at the time will determine how much IFN-γ is produced (Freeman et al., 2012). The authors found IL-12 and IL-18

produced the highest IFN-γ in response when treated with 10 ng/mL of each cytokine in CD8 effectors 8 days post-viral infection hitting between 76.6 and 77.5% whereas IL-12 alone they only saw a modest increase of 14.9% of IFN-γ in unsorted CD8+ cells and even less when IFN-γ CD8+ cells were sorted with only 2.1% IFN-γ detected. (Freeman et al., 2012). Moreover, the CD8+ memory unsorted vs sorted showed similar levels around 31.6% versus 41.3% sorted IFN-γ (Freeman et al., 2012). Authors also showed that stimulating 100 ng/mL was not sufficient to drive responses in CD8+ T-cells with individual cytokines further suggesting the need for at least two signals to activate a T-cell.

In the cytokine stimulation assay, IL-12 alone did not induce IFN-γ yet when in combination with IL-18 led to detectable levels of IFN-γ producing cells by flow cytometry (Figure 14). This further supports the idea that IL-18 acts as a costimulatory cytokine. In this system, due to the lack of activation and costimulatory signal (i.e. α-CD3/α-CD28), cells were pre-exposed to a signal 3 out of order leading to impaired ability to produce IFN-γ and required an additional signal. Unlike the B16F10 co-culture experiment where IL-12 MSA was able to induce some IFN-γ (Figure 12A), there were no tumor antigens available to supply signal 1 in the cytokine stimulation assay because these were all fresh naïve splenocytes. A limitation of this assay was that the IFN-γ produced was significantly greater than that what was seen in the B16F10 co-culture. This is possibly due to the pure population of the cytokine stimulation assay versus the addition of cancer cells making the system more complex. So, the two systems are not directly comparable. In general, *in vitro* assays do not recapitulate the *in vivo* complexities of the tumor microenvironment but offer insight into how we understand systems.

Lastly, it was hypothesized that ICD and pyroptosis may be playing a major role in the release of IL-18 in this system. Pyroptotic cell death is caused by programmed proteolytic activated gasdermin proteins (i.e. Gasdermin D) forming pores on the plasma membrane leading to cell swelling and lysis (Tsuchiya, 2021). It has been shown that IL-1β utilizes gasdermin D pores to exit the cell and be secreted *in vivo* (Heilig et al., 2018). Conventionally, IL-1β and IL-18 share the same pathway by utilizing caspase-1 upon inflammasome activation to become proteolytic cleavage so it is not inconceivable that both cytokines can utilize the same method to exit the cell. Given the results presented in Figure 12, pyroptosis may be responsible for the release of IL-18 from the dual scIL-12 and Full-Length IL-18 arm by caspase-1 followed by a massive production of type I interferon which warrants further investigation to better understand the mechanism of action of this pathway. This effect was dampened when compared to scIL-12 and Active IL-18 containing no signal peptide. But the production of IFN-γ in scIL-12 and Active IL-18 supports the hypothesis that IL-18 is bioactive without needing to undergo proteolytic cleavage. This conclusion is based on the findings in this chapter showing that both IL-12 and IL-18 are needed to drive robust IFN-γ production by upregulation IL-18 receptor.

Chapter V.

Conclusions and Outlook

Based on the findings in Chapter III, IL-18 RNA replicons were validated by gel electrophoresis. Next, model cell lines were chosen to run a pilot study examining if IL-18 can be produced transiently *in vitro* using C2C12 murine myoblasts and RAW264.7 macrophages. Results from the time course ELISAs confirmed IL-18 can be produced, detected, and quantified in a time-dependent fashion. A more translatable delivery method—lipofectamine—was chosen, optimized, and characterized for subsequent studies using mCherry. Following confirmation of efficient nanoparticle-mediated RNA delivery, I quantified responses to the production of transient induced cytokines by ELISA and flow cytometry. These findings support the hypothesis that: 1) IL-18 is bioactive in the absence of a signal peptide; 2) IL-12 and IL-18 replicons synergize; 3) the synergy between IL-12 and IL-18—in the context of RNA replicons—may induce ICD and pyroptosis.

In this thesis, we have expanded the understanding of how IL-18 is produced by the cell and provided evidence that IL-18 can be bioactive without a signal peptide. Armed with this knowledge, one can begin to design more complex systems involving pharmacokinetics by utilizing different forms of IL-18 in cancer cells that are prone to dysregulation of IL-18 like lung cancer and colorectal cancer. One hope is that being able to better control IL-18 production can mitigate side effects associated with it being pleiotropic. IL-18 is already being utilized as a way to augment CAR-T cells to improve production and cytotoxicity (Hu et al., 2017). Moreover, there have been advancements in

generating an IL-18 that has a higher binding affinity to the IL-18 receptor and can escape IL-18 binding protein, the cell's natural IL-18 antagonist (Dinarello et al., 2013; Zhou et al., 2020).

Another example would be the development of tunable switches for spatiotemporal control of protein production in a cell (Chung et al., 2015). This area is of great interest in the field of gene therapy as well as pharmacology and toxicology. A growing field that is in parallel to this idea is the use of protein degraders by utilizing the cell's natural garbage disposal system consisting of an E3 ligase and ubiquitin. Recognition of ubiquitinated proteins via degron sites by E3 ligase leads to effective recruitment of the proteasome and catalyzed degradation of the tagged protein (Lu et al., 2015).

Furthermore, as discussed in Chapter IV, it has been shown that IL-1β utilizes gasdermin D pores to exit the cell and be secreted *in vivo* suggesting a possible exploratory direction using IL-18 RNA replicons to better understand how IL-18 becomes releases from the host cell (Heilig et al., 2018). To further improve understanding of the mechanism associated with proteolytic cleavage of the precursor pro-IL-18 and its release from the host cell, studies conducted in an *in vivo* setting using xenograft implanted cancer cell lines will be informative. Further investigation *in vivo* is needed to confirm the *in vitro* findings covered within the scope of this thesis.

Another important aspect that requires investigation is whether anergy plays as significant of a role as proposed in Chapter IV, which we hypothesized was the reason for the diminished production of an IFN-γ response by IL-12 RNA replicons. One can also hypothesize that IL-18 binding protein may be playing a role along with other inhibitory signals such as IL-10, a pro-survival signal that diminishes pro-inflammatory responses

and preventing IL-18 from co-stimulating with IL-12 during an inflammatory response (Dinarello et al., 2013; Hiraki et al., 2012).

In summary, RNA is making a comeback as a re-emerging technology contributed by the improvements in the field of drug delivery offering a versatile platform to push technological innovation and opening the door to safer next-generation cancer immunotherapies.

References

Abu Bakar, F., & Ng, L. (2018). Nonstructural Proteins of Alphavirus—Potential Targets for Drug Development. *Viruses*, *10*(2), 71. https://doi.org/10.3390/v10020071

Afonina, I. S., Müller, C., Martin, S. J., & Beyaert, R. (2015). Proteolytic Processing of Interleukin-1 Family Cytokines: Variations on a Common Theme. *Immunity*, *42*(6), 991–1004. https://doi.org/10.1016/j.immuni.2015.06.003

Andries, O., Kitada, T., Bodner, K., Sanders, N. N., & Weiss, R. (2015). Synthetic biology devices and circuits for RNA-based 'smart vaccines': A propositional review. *Expert Review of Vaccines*, *14*(2), 313–331. https://doi.org/10.1586/14760584.2015.997714

Arnaud-Barbe, N., Cheynet-Sauvion, V., Oriol, G., Mandrand, B., & Mallet, F. (1998). Transcription of RNA templates by T7 RNA polymerase. *Nucleic Acids Research*, *26*(15), 3550–3554. https://doi.org/10.1093/nar/26.15.3550

Baden, L. R., El Sahly, H. M., Essink, B., Kotloff, K., Frey, S., Novak, R., Diemert, D., Spector, S. A., Rouphael, N., Creech, C. B., McGettigan, J., Khetan, S., Segall, N., Solis, J., Brosz, A., Fierro, C., Schwartz, H., Neuzil, K., Corey, L., … Zaks, T. (2021). Efficacy and Safety of the mRNA-1273 SARS-CoV-2 Vaccine. *New England Journal of Medicine*, *384*(5), 403–416. https://doi.org/10.1056/NEJMoa2035389

Bedard, P. L., Hansen, A. R., Ratain, M. J., & Siu, L. L. (2013). Tumour heterogeneity in the clinic. *Nature*, *501*(7467), 355–364. https://doi.org/10.1038/nature12627

Belouzard, S., Millet, J. K., Licitra, B. N., & Whittaker, G. R. (2012). Mechanisms of Coronavirus Cell Entry Mediated by the Viral Spike Protein. *Viruses*, *4*(6), 1011–1033. https://doi.org/10.3390/v4061011

Blakney, A. K., Ip, S., & Geall, A. J. (2021). An Update on Self-Amplifying mRNA Vaccine Development. *Vaccines*, *9*(2), 97. https://doi.org/10.3390/vaccines9020097

Boraschi, D., & Dinarello, C. A. (2006). IL-18 in autoimmunity: Review. *European Cytokine Network*, *17*(4), 224–252.

Bretscher, P. A. (1999). A two-step, two-signal model for the primary activation of precursor helper T cells. *Proceedings of the National Academy of Sciences*, *96*(1), 185–190. https://doi.org/10.1073/pnas.96.1.185

Brough, D., & Rothwell, N. J. (2007). Caspase-1-dependent processing of pro-interleukin-1β is cytosolic and precedes cell death. *Journal of Cell Science*, *120*(5), 772–781. https://doi.org/10.1242/jcs.03377

Choi, I.-K., Lee, J.-S., Zhang, S.-N., Park, J., Lee, K.-M., Sonn, C. H., & Yun, C.-O. (2011). Oncolytic adenovirus co-expressing IL-12 and IL-18 improves tumor-specific immunity via differentiation of T cells expressing IL-12Rβ2 or IL-18Rα. *Gene Therapy*, *18*(9), 898–909. https://doi.org/10.1038/gt.2011.37

Chow, M. T., Sceneay, J., Paget, C., Wong, C. S. F., Duret, H., Tschopp, J., Möller, A., & Smyth, M. J. (2012). NLRP3 Suppresses NK Cell–Mediated Responses to

Carcinogen-Induced Tumors and Metastases. *Cancer Research*, *72*(22), 5721–5732. https://doi.org/10.1158/0008-5472.CAN-12-0509

Chung, H. K., Jacobs, C. L., Huo, Y., Yang, J., Krumm, S. A., Plemper, R. K., Tsien, R. Y., & Lin, M. Z. (2015). Tunable and reversible drug control of protein production via a self-excising degron. *Nature Chemical Biology*, *11*(9), 713–720. https://doi.org/10.1038/nchembio.1869

Curtsinger, J. M., Schmidt, C. S., Mondino, A., Lins, D. C., Kedl, R. M., Jenkins, M. K., & Mescher, M. F. (1999). Inflammatory Cytokines Provide a Third Signal for Activation of Naive CD4+ and CD8+ T Cells. *The Journal of Immunology*, *162*(6), 3256–3262.

Database resources of the National Center for Biotechnology Information. (2016). *Nucleic Acids Research*, *44*(Database issue), D7–D19. https://doi.org/10.1093/nar/gkv1290

Dinarello, C. A. (1999). IL-18: A TH1 -inducing, proinflammatory cytokine and new member of the IL-1 family. *Journal of Allergy and Clinical Immunology*, *103*(1), 11–24. https://doi.org/10.1016/S0091-6749(99)70518-X

Dinarello, C. A. (2018). Overview of the IL-1 family in innate inflammation and acquired immunity. *Immunological Reviews*, *281*(1), 8–27. https://doi.org/10.1111/imr.12621

Dinarello, C. A., Novick, D., Kim, S., & Kaplanski, G. (2013). Interleukin-18 and IL-18 Binding Protein. *Frontiers in Immunology*, *4*. https://doi.org/10.3389/fimmu.2013.00289

Donahue, N. D., Acar, H., & Wilhelm, S. (2019). Concepts of nanoparticle cellular uptake, intracellular trafficking, and kinetics in nanomedicine. *Advanced Drug Delivery Reviews*, *143*, 68–96. https://doi.org/10.1016/j.addr.2019.04.008

Donahue, N. D., Francek, E. R., Kiyotake, E., Thomas, E. E., Yang, W., Wang, L., Detamore, M. S., & Wilhelm, S. (2020). Assessing nanoparticle colloidal stability with single-particle inductively coupled plasma mass spectrometry (SP-ICP-MS). *Analytical and Bioanalytical Chemistry*, *412*(22), 5205–5216. https://doi.org/10.1007/s00216-020-02783-6

Erdmann, V. A., Barciszewska, M. Z., Hochberg, A., de Groot, N., & Barciszewski, J. (2001). Regulatory RNAs. *Cellular and Molecular Life Sciences CMLS*, *58*(7), 960–977. https://doi.org/10.1007/PL00000913

Freeman, B. E., Hammarlund, E., Raue, H.-P., & Slifka, M. K. (2012). Regulation of innate CD8+ T-cell activation mediated by cytokines. *Proceedings of the National Academy of Sciences*, *109*(25), 9971–9976. https://doi.org/10.1073/pnas.1203543109

Frolov, I., Agapov, E., Hoffman, T. A., Prágai, B. M., Lippa, M., Schlesinger, S., & Rice, C. M. (1999). Selection of RNA Replicons Capable of Persistent Noncytopathic Replication in Mammalian Cells. *Journal of Virology*, *73*(5), 3854–3865. https://doi.org/10.1128/JVI.73.5.3854-3865.1999

Fuller, D. H., & Berglund, P. (2020). Amplifying RNA Vaccine Development. *New England Journal of Medicine*, *382*(25), 2469–2471. https://doi.org/10.1056/NEJMcibr2009737

Gazzinelli, R. T., Hieny, S., Wynn, T. A., Wolf, S., & Sher, A. (1993). Interleukin 12 is required for the T-lymphocyte-independent induction of interferon gamma by an intracellular parasite and induces resistance in T-cell-deficient hosts. *Proceedings of the National Academy of Sciences of the United States of America*, *90*(13), 6115–6119. https://doi.org/10.1073/pnas.90.13.6115

Geall, A. J., Verma, A., Otten, G. R., Shaw, C. A., Hekele, A., Banerjee, K., Cu, Y., Beard, C. W., Brito, L. A., Krucker, T., O'Hagan, D. T., Singh, M., Mason, P. W., Valiante, N. M., Dormitzer, P. R., Barnett, S. W., Rappuoli, R., Ulmer, J. B., & Mandl, C. W. (2012). Nonviral delivery of self-amplifying RNA vaccines. *Proceedings of the National Academy of Sciences*, *109*(36), 14604–14609. https://doi.org/10.1073/pnas.1209367109

Gee, K., Guzzo, C., Che Mat, N. F., Ma, W., & Kumar, A. (2009). The IL-12 family of cytokines in infection, inflammation and autoimmune disorders. *Inflammation & Allergy Drug Targets*, *8*(1), 40–52. https://doi.org/10.2174/187152809787582507

Genentech, Inc. (2021a). *A Phase 1a/1b Open-Label, Dose-Escalation Study of the Safety and Pharmacokinetics of RO7198457 as a Single Agent and in Combination With Atezolizumab in Patients With Locally Advanced or Metastatic Tumors* (Clinical Trial Registration No. NCT03289962). clinicaltrials.gov. https://clinicaltrials.gov/ct2/show/NCT03289962

Genentech, Inc. (2021b). *A Phase II, Open-Label, Multicenter, Randomized Study Of The Efficacy And Safety Of RO7198457 In Combination With Pembrolizumab Versus Pembrolizumab In Patients With Previously Untreated Advanced Melanoma*

(Clinical Trial Registration No. NCT03815058). clinicaltrials.gov. https://clinicaltrials.gov/ct2/show/NCT03815058

Gerdes, N., Sukhova, G. K., Libby, P., Reynolds, R. S., Young, J. L., & Schönbeck, U. (2002). Expression of Interleukin (IL)-18 and Functional IL-18 Receptor on Human Vascular Endothelial Cells, Smooth Muscle Cells, and Macrophages. *Journal of Experimental Medicine*, *195*(2), 245–257. https://doi.org/10.1084/jem.20011022

Ghiringhelli, F., Apetoh, L., Tesniere, A., Aymeric, L., Ma, Y., Ortiz, C., Vermaelen, K., Panaretakis, T., Mignot, G., Ullrich, E., Perfettini, J.-L., Schlemmer, F., Tasdemir, E., Uhl, M., Génin, P., Civas, A., Ryffel, B., Kanellopoulos, J., Tschopp, J., … Zitvogel, L. (2009). Activation of the NLRP3 inflammasome in dendritic cells induces IL-1beta-dependent adaptive immunity against tumors. *Nature Medicine*, *15*(10), 1170–1178. https://doi.org/10.1038/nm.2028

Gould, E., & Solomon, T. (2008). Pathogenic flaviviruses. *The Lancet*, *371*(9611), 500–509. https://doi.org/10.1016/S0140-6736(08)60238-X

Guhaniyogi, J., & Brewer, G. (2001). Regulation of mRNA stability in mammalian cells. *Gene*, *265*(1–2), 11–23. https://doi.org/10.1016/S0378-1119(01)00350-X

Guo, H., Callaway, J. B., & Ting, J. P.-Y. (2015). Inflammasomes: Mechanism of action, role in disease, and therapeutics. *Nature Medicine*, *21*(7), 677–687. https://doi.org/10.1038/nm.3893

He, W., Wan, H., Hu, L., Chen, P., Wang, X., Huang, Z., Yang, Z.-H., Zhong, C.-Q., & Han, J. (2015). Gasdermin D is an executor of pyroptosis and required for

interleukin-1β secretion. *Cell Research*, *25*(12), 1285–1298. https://doi.org/10.1038/cr.2015.139

Heilig, R., Dick, M. S., Sborgi, L., Meunier, E., Hiller, S., & Broz, P. (2018). The Gasdermin-D pore acts as a conduit for IL-1β secretion in mice. *European Journal of Immunology*, *48*(4), 584–592. https://doi.org/10.1002/eji.201747404

Hernandez, R., Brown, D. T., & Paredes, A. (2014). Structural differences observed in arboviruses of the alphavirus and flavivirus genera. *Advances in Virology*, *2014*, 259382. https://doi.org/10.1155/2014/259382

Hiraki, S., Ono, S., Kinoshita, M., Tsujimoto, H., Takahata, R., Miyazaki, H., Saitoh, D., Seki, S., & Hase, K. (2012). Neutralization of IL-10 restores the downregulation of IL-18 receptor on natural killer cells and interferon-γ production in septic mice, thus leading to an improved survival. *Shock (Augusta, Ga.)*, *37*(2), 177–182. https://doi.org/10.1097/SHK.0b013e31823f18ad

Hu, B., Ren, J., Luo, Y., Keith, B., Young, R. M., Scholler, J., Zhao, Y., & June, C. H. (2017). Augmentation of Antitumor Immunity by Human and Mouse CAR T Cells Secreting IL-18. *Cell Reports*, *20*(13), 3025–3033. https://doi.org/10.1016/j.celrep.2017.09.002

Jarret, A., Jackson, R., Duizer, C., Healy, M. E., Zhao, J., Rone, J. M., Bielecki, P., Sefik, E., Roulis, M., Rice, T., Sivanathan, K. N., Zhou, T., Solis, A. G., Honcharova-Biletska, H., Vélez, K., Hartner, S., Low, J. S., Qu, R., de Zoete, M. R., … Flavell, R. A. (2020). Enteric Nervous System-Derived IL-18 Orchestrates Mucosal Barrier Immunity. *Cell*, *180*(1), 50-63.e12. https://doi.org/10.1016/j.cell.2019.12.016

Kim, D. Y., Atasheva, S., McAuley, A. J., Plante, J. A., Frolova, E. I., Beasley, D. W. C., & Frolov, I. (2014). Enhancement of protein expression by alphavirus replicons by designing self-replicating subgenomic RNAs. *Proceedings of the National Academy of Sciences*, *111*(29), 10708–10713. https://doi.org/10.1073/pnas.1408677111

Kittell, B. L., & Helinski, D. R. (1993). Plasmid Incompatibility and Replication Control. In D. B. Clewell (Ed.), *Bacterial Conjugation* (pp. 223–242). Springer US. https://doi.org/10.1007/978-1-4757-9357-4_8

Kobayashi, M., Fitz, L., Ryan, M., Hewick, R. M., Clark, S. C., Chan, S., Loudon, R., Sherman, F., Perussia, B., & Trinchieri, G. (1989). Identification and purification of natural killer cell stimulatory factor (NKSF), a cytokine with multiple biologic effects on human lymphocytes. *The Journal of Experimental Medicine*, *170*(3), 827–845. https://doi.org/10.1084/jem.170.3.827

Kohno, K., Kataoka, J., Ohtsuki, T., Suemoto, Y., Okamoto, I., Usui, M., Ikeda, M., & Kurimoto, M. (1997). IFN-gamma-inducing factor (IGIF) is a costimulatory factor on the activation of Th1 but not Th2 cells and exerts its effect independently of IL-12. *Journal of Immunology (Baltimore, Md.: 1950)*, *158*(4), 1541–1550.

Kutzler, M. A., & Weiner, D. B. (2008). DNA vaccines: Ready for prime time? *Nature Reviews Genetics*, *9*(10), 776–788. https://doi.org/10.1038/nrg2432

Larkin, J., Chiarion-Sileni, V., Gonzalez, R., Grob, J. J., Cowey, C. L., Lao, C. D., Schadendorf, D., Dummer, R., Smylie, M., Rutkowski, P., Ferrucci, P. F., Hill, A., Wagstaff, J., Carlino, M. S., Haanen, J. B., Maio, M., Marquez-Rodas, I.,

McArthur, G. A., Ascierto, P. A., … Wolchok, J. D. (2015). Combined Nivolumab and Ipilimumab or Monotherapy in Untreated Melanoma. *New England Journal of Medicine*, *373*(1), 23–34. https://doi.org/10.1056/NEJMoa1504030

Larkin, J., Chiarion-Sileni, V., Gonzalez, R., Grob, J.-J., Rutkowski, P., Lao, C. D., Cowey, C. L., Schadendorf, D., Wagstaff, J., Dummer, R., Ferrucci, P. F., Smylie, M., Hogg, D., Hill, A., Márquez-Rodas, I., Haanen, J., Guidoboni, M., Maio, M., Schöffski, P., … Wolchok, J. D. (2019). Five-Year Survival with Combined Nivolumab and Ipilimumab in Advanced Melanoma. *New England Journal of Medicine*, *381*(16), 1535–1546. https://doi.org/10.1056/NEJMoa1910836

Leonard, J. P., Sherman, M. L., Fisher, G. L., Buchanan, L. J., Larsen, G., Atkins, M. B., Sosman, J. A., Dutcher, J. P., Vogelzang, N. J., & Ryan, J. L. (1997). Effects of Single-Dose Interleukin-12 Exposure on Interleukin-12–Associated Toxicity and Interferon-γ Production. *Blood*, *90*(7), 2541–2548. https://doi.org/10.1182/blood.V90.7.2541

Li, Y., Su, Z., Zhao, W., Zhang, X., Momin, N., Zhang, C., Wittrup, K. D., Dong, Y., Irvine, D. J., & Weiss, R. (2020). Multifunctional oncolytic nanoparticles deliver self-replicating IL-12 RNA to eliminate established tumors and prime systemic immunity. *Nature Cancer*, *1*(9), 882–893. https://doi.org/10.1038/s43018-020-0095-6

Li, Y., Teague, B., Zhang, Y., Su, Z., Porter, E., Dobosh, B., Wagner, T., Irvine, D. J., & Weiss, R. (2019). In vitro evolution of enhanced RNA replicons for

immunotherapy. *Scientific Reports*, *9*(1), 6932. https://doi.org/10.1038/s41598-019-43422-0

Liu, T., Zhang, L., Joo, D., & Sun, S.-C. (2017). NF-κB signaling in inflammation. *Signal Transduction and Targeted Therapy*, *2*. https://doi.org/10.1038/sigtrans.2017.23

Liu, X., Zhang, Z., Ruan, J., Pan, Y., Magupalli, V. G., Wu, H., & Lieberman, J. (2016). Inflammasome-activated gasdermin D causes pyroptosis by forming membrane pores. *Nature*, *535*(7610), 153–158. https://doi.org/10.1038/nature18629

Liu, Z., Chen, O., Wall, J. B. J., Zheng, M., Zhou, Y., Wang, L., Ruth Vaseghi, H., Qian, L., & Liu, J. (2017). Systematic comparison of 2A peptides for cloning multi-genes in a polycistronic vector. *Scientific Reports*, *7*. https://doi.org/10.1038/s41598-017-02460-2

Lodish, H., Berk, A., Zipursky, S. L., Matsudaira, P., Baltimore, D., & Darnell, J. (2000). The Three Roles of RNA in Protein Synthesis. *Molecular Cell Biology. 4th Edition*. https://www.ncbi.nlm.nih.gov/books/NBK21603/

Lu, J., Qian, Y., Altieri, M., Dong, H., Wang, J., Raina, K., Hines, J., Winkler, J. D., Crew, A. P., Coleman, K., & Crews, C. M. (2015). Hijacking the E3 Ubiquitin Ligase Cereblon to Efficiently Target BRD4. *Chemistry & Biology*, *22*(6), 755–763. https://doi.org/10.1016/j.chembiol.2015.05.009

Lundstrom, K. (2014). Alphavirus-Based Vaccines. *Viruses*, *6*(6), 2392–2415. https://doi.org/10.3390/v6062392

Lundstrom, K. (2018). Self-Replicating RNA Viruses for RNA Therapeutics. *Molecules*, *23*(12), 3310. https://doi.org/10.3390/molecules23123310

McCullough, K., Milona, P., Thomann-Harwood, L., Démoulins, T., Englezou, P., Suter, R., & Ruggli, N. (2014). Self-Amplifying Replicon RNA Vaccine Delivery to Dendritic Cells by Synthetic Nanoparticles. *Vaccines*, *2*(4), 735–754. https://doi.org/10.3390/vaccines2040735

Melo, M., Porter, E., Zhang, Y., Silva, M., Li, N., Dobosh, B., Liguori, A., Skog, P., Landais, E., Menis, S., Sok, D., Nemazee, D., Schief, W. R., Weiss, R., & Irvine, D. J. (2019). Immunogenicity of RNA Replicons Encoding HIV Env Immunogens Designed for Self-Assembly into Nanoparticles. *Molecular Therapy*, *27*(12), 2080–2090. https://doi.org/10.1016/j.ymthe.2019.08.007

Melton, D. A., Krieg, P. A., Rebagliati, M. R., Maniatis, T., Zinn, K., & Green, M. R. (1984). Efficient *in vitro* synthesis of biologically active RNA and RNA hybridization probes from plasmids containing a bacteriophage SP6 promoter. *Nucleic Acids Research*, *12*(18), 7035–7056. https://doi.org/10.1093/nar/12.18.7035

Momin, N., Mehta, N. K., Bennett, N. R., Ma, L., Palmeri, J. R., Chinn, M. M., Lutz, E. A., Kang, B., Irvine, D. J., Spranger, S., & Wittrup, K. D. (2019). Anchoring of intratumorally administered cytokines to collagen safely potentiates systemic cancer immunotherapy. *Science Translational Medicine*, *11*(498). https://doi.org/10.1126/scitranslmed.aaw2614

Moynihan, K. D. (Kelly D. (2017). *Engineering immunity: Enhancing T Cell vaccines and combination immunotherapies for the treatment of cancer* [Thesis, Massachusetts Institute of Technology]. https://dspace.mit.edu/handle/1721.1/113960

Nakahira, M., Ahn, H.-J., Park, W.-R., Gao, P., Tomura, M., Park, C.-S., Hamaoka, T., Ohta, T., Kurimoto, M., & Fujiwara, H. (2002). Synergy of IL-12 and IL-18 for IFN-γ Gene Expression: IL-12-Induced STAT4 Contributes to IFN-γ Promoter Activation by Up-Regulating the Binding Activity of IL-18-Induced Activator Protein 1. *The Journal of Immunology*, *168*(3), 1146–1153. https://doi.org/10.4049/jimmunol.168.3.1146

Nakamura, K., Okamura, H., Wada, M., Nagata, K., & Tamura, T. (1989). Endotoxin-induced serum factor that stimulates gamma interferon production. *Infection and Immunity*, *57*(2), 590–595. https://doi.org/10.1128/IAI.57.2.590-595.1989

Nakamura, S., Otani, T., Ijiri, Y., Motoda, R., Kurimoto, M., & Orita, K. (2000). IFN-γ-Dependent and -Independent Mechanisms in Adverse Effects Caused by Concomitant Administration of IL-18 and IL-12. *The Journal of Immunology*, *164*(6), 3330–3336. https://doi.org/10.4049/jimmunol.164.6.3330

Nakanishi, K. (2018). Unique Action of Interleukin-18 on T Cells and Other Immune Cells. *Frontiers in Immunology*, *9*. https://doi.org/10.3389/fimmu.2018.00763

Okamura, H., Tsutsui, H., Komatsu, T., Yutsudo, M., Hakura, A., Tanimoto, T., Torigoe, K., Okura, T., Nukada, Y., Hattori, K., Akita, K., Namba, M., Tanabe, F., Konishi, K., Fukuda, S., & Kurimoto, M. (1995). Cloning of a new cytokine that induces IFN-γ production by T cells. *Nature*, *378*(6552), 88–91. https://doi.org/10.1038/378088a0

Omoto, Y., Tokime, K., Yamanaka, K., Habe, K., Morioka, T., Kurokawa, I., Tsutsui, H., Yamanishi, K., Nakanishi, K., & Mizutani, H. (2006). Human Mast Cell Chymase Cleaves Pro-IL-18 and Generates a Novel and Biologically Active IL-18

Fragment. *The Journal of Immunology*, *177*(12), 8315–8319. https://doi.org/10.4049/jimmunol.177.12.8315

Pardi, N., Tuyishime, S., Muramatsu, H., Kariko, K., Mui, B. L., Tam, Y. K., Madden, T. D., Hope, M. J., & Weissman, D. (2015). Expression kinetics of nucleoside-modified mRNA delivered in lipid nanoparticles to mice by various routes. *Journal of Controlled Release : Official Journal of the Controlled Release Society*, *217*, 345–351. https://doi.org/10.1016/j.jconrel.2015.08.007

Park, K. S., Sun, X., Aikins, M. E., & Moon, J. J. (2021). Non-viral COVID-19 vaccine delivery systems. *Advanced Drug Delivery Reviews*, *169*, 137–151. https://doi.org/10.1016/j.addr.2020.12.008

Pascolo, S. (2008). Vaccination with Messenger RNA (mRNA). In S. Bauer & G. Hartmann (Eds.), *Toll-Like Receptors (TLRs) and Innate Immunity* (pp. 221–235). Springer. https://doi.org/10.1007/978-3-540-72167-3_11

Polack, F. P., Thomas, S. J., Kitchin, N., Absalon, J., Gurtman, A., Lockhart, S., Perez, J. L., Pérez Marc, G., Moreira, E. D., Zerbini, C., Bailey, R., Swanson, K. A., Roychoudhury, S., Koury, K., Li, P., Kalina, W. V., Cooper, D., Frenck, R. W., Hammitt, L. L., … Gruber, W. C. (2020). Safety and Efficacy of the BNT162b2 mRNA Covid-19 Vaccine. *New England Journal of Medicine*, *383*(27), 2603–2615. https://doi.org/10.1056/NEJMoa2034577

Rickles, R. J., Darrow, A. L., & Strickland, S. (1988). Molecular cloning of complementary DNA to mouse tissue plasminogen activator mRNA and its expression during F9 teratocarcinoma cell differentiation. *Journal of Biological Chemistry*, *263*(3), 1563–1569. https://doi.org/10.1016/S0021-9258(19)57341-0

Rong, M., He, B., McAllister, W. T., & Durbin, R. K. (1998). Promoter specificity determinants of T7 RNA polymerase. *Proceedings of the National Academy of Sciences*, *95*(2), 515–519. https://doi.org/10.1073/pnas.95.2.515

Schulz, E. G., Mariani, L., Radbruch, A., & Höfer, T. (2009). Sequential polarization and imprinting of type 1 T helper lymphocytes by interferon-gamma and interleukin-12. *Immunity*, *30*(5), 673–683. https://doi.org/10.1016/j.immuni.2009.03.013

Sckisel, G. D., Bouchlaka, M. N., Monjazeb, A. M., Crittenden, M., Curti, B. D., Wilkins, D. E. C., Alderson, K. A., Sungur, C. M., Ames, E., Mirsoian, A., Reddy, A., Alexander, W., Soulika, A., Blazar, B. R., Longo, D. L., Wiltrout, R. H., & Murphy, W. J. (2015). Out-of-Sequence Signal 3 Paralyzes Primary CD4+ T-Cell-Dependent Immunity. *Immunity*, *43*(2), 240–250. https://doi.org/10.1016/j.immuni.2015.06.023

Seki, E., Tsutsui, H., Nakano, H., Tsuji, N. M., Hoshino, K., Adachi, O., Adachi, K., Futatsugi, S., Kuida, K., Takeuchi, O., Okamura, H., Fujimoto, J., Akira, S., & Nakanishi, K. (2001). Lipopolysaccharide-Induced IL-18 Secretion from Murine Kupffer Cells Independently of Myeloid Differentiation Factor 88 That Is Critically Involved in Induction of Production of IL-12 and IL-1β. *The Journal of Immunology*, *166*(4), 2651–2657. https://doi.org/10.4049/jimmunol.166.4.2651

Slusarczyk, A. L., Lin, A., & Weiss, R. (2012). Foundations for the design and implementation of synthetic genetic circuits. *Nature Reviews Genetics*, *13*(6), 406–420. https://doi.org/10.1038/nrg3227

Tang, A., & Harding, F. (2019). The challenges and molecular approaches surrounding interleukin-2-based therapeutics in cancer. *Cytokine: X*, *1*(1), 100001. https://doi.org/10.1016/j.cytox.2018.100001

Tominaga, K., Yoshimoto, T., Torigoe, K., Kurimoto, M., Matsui, K., Hada, T., Okamura, H., & Nakanishi, K. (2000). IL-12 synergizes with IL-18 or IL-1β for IFN-γ production from human T cells. *International Immunology*, *12*(2), 151–160. https://doi.org/10.1093/intimm/12.2.151

Trinchieri, G. (1998). Immunobiology of lnterleukin-12. *Immunologic Research*, *17*(1–2), 269–278. https://doi.org/10.1007/BF02786451

Tsuchiya, K. (2021). Switching from Apoptosis to Pyroptosis: Gasdermin-Elicited Inflammation and Antitumor Immunity. *International Journal of Molecular Sciences*, *22*(1). https://doi.org/10.3390/ijms22010426

Tuittila, M. T., Santagati, M. G., Röyttä, M., Määttä, J. A., & Hinkkanen, A. E. (2000). Replicase Complex Genes of Semliki Forest Virus Confer Lethal Neurovirulence. *Journal of Virology*, *74*(10), 4579–4589. https://doi.org/10.1128/JVI.74.10.4579-4589.2000

Uversky, V. N., & Longhi, S. (Eds.). (2011). *Flexible Viruses: Structural Disorder in Viral Proteins*. John Wiley & Sons, Inc. https://doi.org/10.1002/9781118135570

Varnavski, A. N., Young, P. R., & Khromykh, A. A. (2000). Stable High-Level Expression of Heterologous Genes In Vitro and In Vivo by Noncytopathic DNA-Based Kunjin Virus Replicon Vectors. *Journal of Virology*, *74*(9), 4394–4403. https://doi.org/10.1128/JVI.74.9.4394-4403.2000

Vignali, D. A. A., & Kuchroo, V. K. (2012). IL-12 family cytokines: Immunological playmakers. *Nature Immunology*, *13*(8), 722–728. https://doi.org/10.1038/ni.2366

Vogel, A. B., Lambert, L., Kinnear, E., Busse, D., Erbar, S., Reuter, K. C., Wicke, L., Perkovic, M., Beissert, T., Haas, H., Reece, S. T., Sahin, U., & Tregoning, J. S. (2018). Self-Amplifying RNA Vaccines Give Equivalent Protection against Influenza to mRNA Vaccines but at Much Lower Doses. *Molecular Therapy*, *26*(2), 446–455. https://doi.org/10.1016/j.ymthe.2017.11.017

Wadhwa, A., Aljabbari, A., Lokras, A., Foged, C., & Thakur, A. (2020). Opportunities and Challenges in the Delivery of mRNA-Based Vaccines. *Pharmaceutics*, *12*(2). https://doi.org/10.3390/pharmaceutics12020102

Wagner, T. E., Becraft, J. R., Bodner, K., Teague, B., Zhang, X., Woo, A., Porter, E., Alburquerque, B., Dobosh, B., Andries, O., Sanders, N. N., Beal, J., Densmore, D., Kitada, T., & Weiss, R. (2018). Small-molecule-based regulation of RNA-delivered circuits in mammalian cells. *Nature Chemical Biology*, *14*(11), 1043–1050. https://doi.org/10.1038/s41589-018-0146-9

Wallenstein, E. J., Barminko, J., Schloss, R. S., & Yarmush, M. L. (2010). Serum Starvation Improves Transient Transfection Efficiency in Differentiating Embryonic Stem Cells. *Biotechnology Progress*, *26*(6), 1714–1723. https://doi.org/10.1002/btpr.472

WHO Coronavirus (COVID-19) Dashboard. (n.d.). Retrieved March 10, 2021, from https://covid19.who.int

Yoshimoto, T., Takeda, K., Tanaka, T., Ohkusu, K., Kashiwamura, S., Okamura, H., Akira, S., & Nakanishi, K. (1998). IL-12 Up-Regulates IL-18 Receptor

Expression on T Cells, Th1 Cells, and B Cells: Synergism with IL-18 for IFN-γ Production. *The Journal of Immunology*, *161*(7), 3400–3407.

Zaki, M. H., Boyd, K. L., Vogel, P., Kastan, M. B., Lamkanfi, M., & Kanneganti, T.-D. (2010). The NLRP3 inflammasome protects against loss of epithelial integrity and mortality during experimental colitis. *Immunity*, *32*(3), 379–391. https://doi.org/10.1016/j.immuni.2010.03.003

Zhang, C., Maruggi, G., Shan, H., & Li, J. (2019). Advances in mRNA Vaccines for Infectious Diseases. *Frontiers in Immunology*, *10*. https://doi.org/10.3389/fimmu.2019.00594

Zhang, F., Parayath, N. N., Ene, C. I., Stephan, S. B., Koehne, A. L., Coon, M. E., Holland, E. C., & Stephan, M. T. (2019). Genetic programming of macrophages to perform anti-tumor functions using targeted mRNA nanocarriers. *Nature Communications*, *10*(1), 3974. https://doi.org/10.1038/s41467-019-11911-5

Zhou, T., Damsky, W., Weizman, O.-E., McGeary, M. K., Hartmann, K. P., Rosen, C. E., Fischer, S., Jackson, R., Flavell, R. A., Wang, J., Sanmamed, M. F., Bosenberg, M. W., & Ring, A. M. (2020). IL-18BP is a secreted immune checkpoint and barrier to IL-18 immunotherapy. *Nature*, *583*(7817), 609–614. https://doi.org/10.1038/s41586-020-2422-6